IMAGING IN RANDOMLY LAYERED MEDIA BY CROSS-CORRELATING NOISY SIGNALS

JOSSELIN GARNIER*

Abstract. We consider an active source embedded in a randomly layered medium. We study the cross-correlation functions of the signals recorded at a series of points located at the surface. We show that this information can be processed to locate the source inside the medium. The analysis is based on a separation of scales technique and limit theorems for random differential equations. The statistical stability of the imaging method is proved. The analogy with the time-reversal of waves is enlightened, but the main difference is also put forward: we propose a passive way of imaging an unknown medium without the use of any active device. We finally extend these ideas for the location of a scatterer illuminated by a controlled source located at the surface or by a set of unknown sources generating random noise.

Key words. Acoustic waves, random media, asymptotic theory.

AMS subject classifications. 76B15, 35Q99, 60F05.

1. Introduction. Imaging in complex media is a difficult but exciting problem, with many potential applications [30]. We consider the problem of the source localization when the source is embedded in a randomly layered half-space. We study the statistical properties of the signals recorded at the surface. We focus our attention on the cross-correlation function between the signals recorded at two observation points. From the exact statistical description of this function, we propose a way to recover the precise location of the source from a data set consisting of the signals recorded at five (or more) observation points. We then extend this technique to the case of a point scatterer embedded in the random half-space and illuminated by a known or unknown source, or by a set of known or unknown sources.

The waves recorded at the observation points have scattered from the random heterogeneities of the medium. We shall first consider configurations where a coherent front pulse can be detected. According to the O'Doherty Anstey theory [24], this front pulse is spread out and shifted due to multiple scattering. In particular a random time shift makes it difficult to recover precise information about travel times. We shall also consider configurations where the signal arriving at the surface is so noisy that no coherent or ballistic front can be detected. Information about an individual scatterer could be understood to be lost in such a case. However time-reversal experiments [15, 16] and the explanations by Clouet and Fouque [11] extended by Papanicolaou *et al.* of the self-averaging property of time-reversal for broadband signals [5, 3] have shown that multiple scattering is not always a nuisance. The utility of time-reversal for imaging has been pointed out recently [6, 17]. Unfortunately it is not always possible to perform real time-reversal experiments, in geophysics for instance, as it requires very specific active devices. In this paper we shall see that cross-correlation functions of recorded noisy signals are useful to image a random medium. The first mathematical guess is that a cross-correlation function is in some sense close to achieve a time reversal experiment [35, 26], as it involves the product of two Green's functions, one of them being complex-conjugated.

We should mention that the idea to exploit the cross-correlation of noisy signals to retrieve information about ballistic wave motion has first been proposed in seismology

*Laboratoire de Statistique et Probabilités, Université Paul Sabatier, 118 Route de Narbonne, 31062 Toulouse Cedex 4, France, garnier@cict.fr

and helio-seismology [25, 13]. First explanations and conditions of applicability are proposed and criticized by physicists [8, 22, 31]. Using recent tools developed for the analysis of time-reversal experiments, we are able to give more mathematical insight into this issue and to enlighten the key points. In particular, we shall see that the source needs to be broadband to ensure the statistical self-averaging property.

In the regime of separation of scales a framework for the analysis of acoustic waves propagating in randomly layered media has been set forth in [1]. The scale regime we consider corresponds to wavelengths that are large relative to the correlation length of the medium, but short relative to the depth of the source. We consider linear acoustic waves propagating in three spatial dimensions

$$\rho \frac{\partial \vec{\mathbf{u}}}{\partial t} + \nabla p = \vec{\mathbf{F}}, \tag{1.1}$$

$$\frac{1}{K}\frac{\partial p}{\partial t} + \nabla \cdot \vec{\mathbf{u}} = 0, \tag{1.2}$$

where p is the pressure, $\vec{\mathbf{u}}$ is the velocity, ρ is the density of the medium, and K the bulk modulus. The forcing term $\vec{\mathbf{F}}$ is due to the source. In this paper the three-dimensional spatial variable is denoted by $\vec{\mathbf{r}} = (\mathbf{x}, z)$, where we distinguish the transverse spatial coordinates $\mathbf{x} = (x, y)$ and the longitudinal coordinate z. We assume that the density is constant and the bulk modulus is randomly fluctuating along the z-coordinate only in the slab $(-L, 0)$. Note that we can choose L large enough so that the termination of the slab does not affect the wave field at the surface $z = 0$ over the time window that we consider. More explicitly, the coefficients of the medium are described by

$$\rho \equiv \rho_0, \tag{1.3}$$

$$\frac{1}{K} = \begin{cases} \dfrac{1}{K_0}\left(1 + \nu(\dfrac{z}{\varepsilon^2})\right) & \text{if } -L < z < 0, \\ \dfrac{1}{K_0} & \text{if } z > 0 \text{ or } z < -L, \end{cases} \tag{1.4}$$

where ν is a zero-mean mixing process and ε^2 is a small dimensionless parameter that characterizes the ratio between the correlation length of the medium and the typical depth of the source. Note that the fluctuations of the medium are not assumed to be small. The average velocity is given by $c_0 = \sqrt{K_0/\rho_0}$. A point source located at $(\mathbf{x}_s, z_s)$, $z_s < 0$, generates a forcing term $\vec{\mathbf{F}}$ (see Figure 1.1)

$$\vec{\mathbf{F}}(t, \mathbf{x}, z) = \vec{\mathbf{f}}^{\varepsilon}(t)\delta(\mathbf{x} - \mathbf{x}_s)\delta(z - z_s). \tag{1.5}$$

We shall first address the case where the source emits a short pulse at time t_s:

$$\vec{\mathbf{f}}^{\varepsilon}(t) = \begin{pmatrix} \mathbf{f}_{\mathbf{x}} \\ f_z \end{pmatrix} (\frac{t - t_s}{\varepsilon}). \tag{1.6}$$

The time duration of the source is scaled by ε which is large compared to the correlation length of the medium (of order ε^2) and small compared to the travel times between the source and the observation points (of order 1).

We shall also address the case where the point source emits a stationary random signal with Gaussian statistics

$$\vec{\mathbf{f}}^{\varepsilon}(t) = \varepsilon^{\frac{1}{2}} \begin{pmatrix} \mathbf{f}_{\mathbf{x}} \\ f_z \end{pmatrix} (\frac{t}{\varepsilon}). \tag{1.7}$$

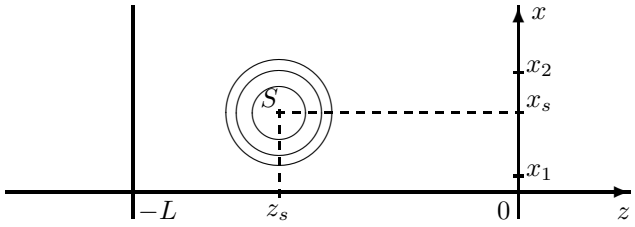

FIG. 1.1. *Emission from a point source. The signal is recorded at different observation points* $O_1 = (\mathbf{x}_1, 0)$, $O_2 = (\mathbf{x}_2, 0)$,... *distributed at the surface* $z = 0$.

characterized by its autocorrelation matrix

$$\mathcal{G}(t) = \left(\langle f_i(0) f_j(t)\rangle\right)_{i,j\in\{x,y,z\}},$$

where $\langle\cdot\rangle$ stands for an averaging with respect to the statistical distribution of the source. Note that the amplitude factor $\varepsilon^{\frac{1}{2}}$ has no importance since the propagation equations are linear. This factor has been added to ensure that the energy released by the source during a time interval of order 1 is of the same order as in the case of the short pulse (1.6). The power spectral density matrix $\hat{\mathcal{G}}(\omega)$ of the signal $\vec{\mathbf{f}}$ is equal to the Fourier transform of the autocorrelation matrix of the stationary process f

$$\hat{\mathcal{G}}(\omega) = \int \mathcal{G}(t) e^{-i\omega t} dt.$$

It is a non-negative definite matrix. Its entries are even, real-valued functions because $\mathcal{G}_{ij}$ are even, real-valued functions. We shall assume that $\omega \mapsto \omega^2 |\hat{\mathcal{G}}(\omega)|$ belongs to L^1. As a consequence of the Bochner theorem, the process $\vec{\mathbf{f}}$ can be represented as the stochastic integral

$$\vec{\mathbf{f}}(t) = \frac{1}{\sqrt{2\pi}} \int e^{i\omega t} \hat{g}(\omega) d\vec{\mathbf{W}}_\omega, \tag{1.8}$$

where $\hat{g}$ is a square root of $\hat{\mathcal{G}}$, i.e. a 3×3 matrix such that $\hat{g}(\omega)^T \hat{g}(\omega) = \hat{\mathcal{G}}(\omega)$. $\vec{\mathbf{W}}_\omega$ is a $\mathbb{C}^3$-valued Gaussian process

$$\vec{\mathbf{W}}_\omega = \frac{\vec{\mathbf{W}}^1_\omega + \vec{\mathbf{W}}^1_{-\omega}}{2} + i \frac{\vec{\mathbf{W}}^2_\omega - \vec{\mathbf{W}}^2_{-\omega}}{2},$$

where $\vec{\mathbf{W}}^1$ and $\vec{\mathbf{W}}^2$ are two independent three-dimensional Brownian motions. Note that $\vec{\mathbf{W}}_\omega$ satisfies $\overline{\vec{\mathbf{W}}_\omega} = \vec{\mathbf{W}}_{-\omega}$ and $\left\langle dW_{i\omega} d\overline{W_{j\omega'}} \right\rangle = \delta_{ij}\delta(\omega - \omega') d\omega d\omega'$.

In Section 2 we derive an integral representation for the field at the surface. The integral representation is obtained by taking a Fourier transform in the time and lateral space coordinates. This reduces the problem to a family of one dimensional problems that can be analyzed by decomposing the wave field into right and left going waves. In Section 4 we address the case where the point source emits a short pulse. We study the propagation of the front pulse and show that the random arrival times of the front pulses at five (or more) observation points are sufficient to detect the source location without any error. In Section 5 we consider the case of a stationary source signal. We carry out a careful stationary phase analysis combined with standard diffusion approximation results in the limit of ε small. This gives a stochastic limit

for the cross-correlation function of the recorded field. The explicit expressions allow us to remove the random part and to propose a procedure to get the source location without any error. Finally in Section 6 we revisit our analysis in the case of an embedded scatterer illuminated by a source or a set of sources located at the surface.

2. The integral representation of the field.

2.1. Emission of a short pulse from a point source. In the scaling that we consider the typical wavelength of the source is of order ε and we use the following specific Fourier transform and its inverse with respect to the time and the transverse spatial coordinates

$$\hat{p}(\omega,\boldsymbol{\kappa},z) = \int\int p(t,\mathbf{x},z) e^{i\frac{\omega}{\varepsilon}(t-\boldsymbol{\kappa}\cdot\mathbf{x})} dt d\mathbf{x},$$
$$p(t,\mathbf{x},z) = \frac{1}{(2\pi\varepsilon)^3}\int\int \hat{p}(\omega,\boldsymbol{\kappa},z) e^{-i\frac{\omega}{\varepsilon}(t-\boldsymbol{\kappa}\cdot\mathbf{x})}\omega^2 d\omega d\boldsymbol{\kappa}.$$

Taking the scaled Fourier transform gives that $\hat{\tilde{\mathbf{u}}} = (\hat{\mathbf{v}}, \hat{u})$ and $\hat{p}$ satisfy the system

$$-\rho_0 \frac{i\omega}{\varepsilon}\hat{\mathbf{v}} + i\frac{\omega}{\varepsilon}\boldsymbol{\kappa}\hat{p} = \varepsilon \hat{\mathbf{f}}_{\mathbf{x}}(\omega) e^{i\frac{\omega}{\varepsilon}(t_s-\boldsymbol{\kappa}\cdot\mathbf{x}_s)}\delta(z-z_s), \tag{2.1}$$

$$-\rho_0 \frac{i\omega}{\varepsilon}\hat{u} + \frac{\partial \hat{p}}{\partial z} = \varepsilon \hat{f}_z(\omega) e^{i\frac{\omega}{\varepsilon}(t_s-\boldsymbol{\kappa}\cdot\mathbf{x}_s)}\delta(z-z_s), \tag{2.2}$$

$$-\frac{1}{K(z)}\frac{i\omega}{\varepsilon}\hat{p} + i\frac{\omega}{\varepsilon}\boldsymbol{\kappa}\cdot\hat{\mathbf{v}} + \frac{\partial \hat{u}}{\partial z} = 0, \tag{2.3}$$

where $\hat{f}$ is the ordinary unscaled Fourier transform of the pulse profile

$$\hat{f}(\omega) = \int f(t) e^{i\omega t} dt, \qquad f(t) = \frac{1}{2\pi}\int \hat{f}(\omega) e^{-i\omega t} d\omega.$$

We deduce that $(\hat{u},\hat{p})$ satisfy the following closed system for $-L < z < z_s$ and $z_s < z < 0$

$$\frac{\partial \hat{u}}{\partial z} + \frac{i\omega}{\varepsilon}\left(-\frac{1}{K(z)} + \frac{|\boldsymbol{\kappa}|^2}{\rho_0}\right)\hat{p} = 0, \tag{2.4}$$

$$\frac{\partial \hat{p}}{\partial z} - \frac{i\omega}{\varepsilon}\rho_0 \hat{u} = 0, \tag{2.5}$$

with the jumps at $z = z_s$ given by

$$[\hat{u}]_{z_s} := \hat{u}(\omega,\boldsymbol{\kappa},z_s^+) - \hat{u}(\omega,\boldsymbol{\kappa},z_s^-) = \varepsilon \frac{\boldsymbol{\kappa}\cdot\hat{\mathbf{f}}_{\mathbf{x}}(\omega)}{\rho_0} e^{i\frac{\omega}{\varepsilon}(t_s-\boldsymbol{\kappa}\cdot\mathbf{x}_s)}, \tag{2.6}$$

$$[\hat{p}]_{z_s} := \hat{p}(\omega,\boldsymbol{\kappa},z_s^+) - \hat{p}(\omega,\boldsymbol{\kappa},z_s^-) = \varepsilon \hat{f}_z(\omega) e^{i\frac{\omega}{\varepsilon}(t_s-\boldsymbol{\kappa}\cdot\mathbf{x}_s)}. \tag{2.7}$$

We introduce the right and left propagating wave modes a and b which are defined by

$$\hat{p}(\omega,\boldsymbol{\kappa},z) = \frac{\sqrt{I_0(\kappa)}}{2}\left(a(\omega,\boldsymbol{\kappa},z)e^{i\frac{\omega}{\varepsilon}\zeta_0(\kappa)z} - b(\omega,\boldsymbol{\kappa},z)e^{-i\frac{\omega}{\varepsilon}\zeta_0(\kappa)z}\right), \tag{2.8}$$

$$\hat{u}(\omega,\boldsymbol{\kappa},z) = \frac{1}{2\sqrt{I_0(\kappa)}}\left(a(\omega,\boldsymbol{\kappa},z)e^{i\frac{\omega}{\varepsilon}\zeta_0(\kappa)z} + b(\omega,\boldsymbol{\kappa},z)e^{-i\frac{\omega}{\varepsilon}\zeta_0(\kappa)z}\right), \tag{2.9}$$

where $\kappa = |\boldsymbol{\kappa}|$, $\zeta_0^{-1}(\kappa)$ is the average longitudinal velocity and $I_0(\kappa)$ is the acoustic impedance:

$$\zeta_0(\kappa) = \frac{\sqrt{1 - c_0^2\kappa^2}}{c_0}, \qquad I_0(\kappa) = \frac{\rho_0}{\zeta_0(\kappa)}.$$

Here we only consider propagating modes and ignore evanescent modes meaning that $\kappa < c_0^{-1}$. The system for a and b can be written as

$$\frac{\partial}{\partial z}\begin{pmatrix} a \\ b \end{pmatrix}(\omega,\kappa,z) = Q^\varepsilon(\omega,\kappa,z)\begin{pmatrix} a \\ b \end{pmatrix}(\omega,\kappa,z) \tag{2.10}$$

where the complex 2×2 matrix Q^ε is given by:

$$Q^\varepsilon(\omega,\kappa,z) = \frac{i\omega\zeta_0(\kappa)}{2\varepsilon(1-c_0^2\kappa^2)}\nu(\frac{z}{\varepsilon^2})\begin{pmatrix} 1 & -e^{\frac{-2i\omega\zeta_0(\kappa)z}{\varepsilon}} \\ e^{\frac{2i\omega\zeta_0(\kappa)z}{\varepsilon}} & -1 \end{pmatrix}. \tag{2.11}$$

Using the definitions (2.8) and (2.9) of a and b and the expressions (2.6) and (2.7) for the jumps in $\hat{u}$ and $\hat{p}$ we deduce the jumps at $z = z_s$ for the modes a and b

$$[a]_{z_s} = \varepsilon e^{i\frac{\omega}{\varepsilon}(t_s - \boldsymbol{\kappa}\cdot\mathbf{x}_s - \zeta_0(\kappa)z_s)} S_a(\omega,\boldsymbol{\kappa}), \tag{2.12}$$

$$[b]_{z_s} = \varepsilon e^{i\frac{\omega}{\varepsilon}(t_s - \boldsymbol{\kappa}\cdot\mathbf{x}_s + \zeta_0(\kappa)z_s)} S_b(\omega,\boldsymbol{\kappa}), \tag{2.13}$$

with the source contributions given by

$$S_a(\omega,\boldsymbol{\kappa}) = \frac{\sqrt{I_0(\kappa)}}{\rho_0}\boldsymbol{\kappa}\cdot\hat{\mathbf{f}}_{\mathbf{x}}(\omega) + \frac{1}{\sqrt{I_0(\kappa)}}\hat{f}_z(\omega), \tag{2.14}$$

$$S_b(\omega,\boldsymbol{\kappa}) = \frac{\sqrt{I_0(\kappa)}}{\rho_0}\boldsymbol{\kappa}\cdot\hat{\mathbf{f}}_{\mathbf{x}}(\omega) - \frac{1}{\sqrt{I_0(\kappa)}}\hat{f}_z(\omega). \tag{2.15}$$

The system for a and b is completed by the boundary conditions at $z = 0$ and $z = -L$ that are shown in Figure 2.1. We assume that no energy is coming from $+\infty$ and $-\infty$, so that we get the radiation conditions

$$a(\omega,\boldsymbol{\kappa},-L) = 0, \qquad b(\omega,\boldsymbol{\kappa},0) = 0.$$

The quantity of interest is the wave field at the surface which is completely characterized by $a(\omega,\boldsymbol{\kappa},0)$ since $b(\omega,\boldsymbol{\kappa},0) = 0$.

We transform this boundary value problem into an initial value problem by introducing the propagator $Y(\omega,\kappa,z_0,z)$, $-L \le z_0 \le z \le 0$, which is a family of complex 2×2 matrices solutions of

$$\frac{\partial Y}{\partial z} = Q^\varepsilon(\omega,\kappa,z)Y, \qquad Y(\omega,\kappa,z_0,z=z_0) = \mathrm{Id}_{\mathbb{C}^2}.$$

By using the particular form of the matrix Q^ε in (2.11) we can show that if the column vector $(\alpha,\beta)^T$ is solution of equation (2.10) with the initial conditions

$$\alpha(z_0,z=z_0) = 1, \qquad \beta(z_0,z=z_0) = 0, \tag{2.16}$$

then the column vector $(\overline{\beta},\overline{\alpha})^T$ is another solution linearly independent of the first solution, so that the propagator matrix Y can be written as

$$Y(z_0,z) = \begin{pmatrix} \alpha & \overline{\beta} \\ \beta & \overline{\alpha} \end{pmatrix}(z_0,z).$$

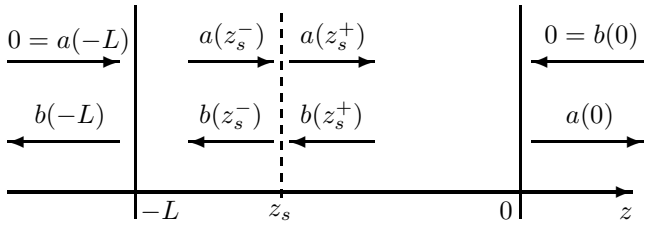

FIG. 2.1. *Boundary conditions at $z = -L$ and $z = 0$ corresponding to the emission from the point source located at depth z_s.*

The boundary conditions at $z = -L$ and $z = 0$ then imply

$$Y(-L, z_s) \begin{pmatrix} 0 \\ b(-L) \end{pmatrix} = \begin{pmatrix} a(z_s^-) \\ b(z_s^-) \end{pmatrix}, \quad Y(z_s, 0) \begin{pmatrix} a(z_s^+) \\ b(z_s^+) \end{pmatrix} = \begin{pmatrix} a(0) \\ 0 \end{pmatrix}. \tag{2.17}$$

The system determined by (2.12,2.13,2.17) whose unknown are $b(-L)$ and $a(0)$ can be solved, and we get:

$$\begin{aligned} a(\omega, \boldsymbol{\kappa}, 0) = \varepsilon e^{i\frac{\omega}{\varepsilon}(t_s - \boldsymbol{\kappa}\cdot\mathbf{x}_s)} \Big[& e^{-i\frac{\omega}{\varepsilon}\zeta_0(\kappa) z_s} T_g(\omega, \kappa, z_s) S_a(\omega, \boldsymbol{\kappa}) \\ & + e^{i\frac{\omega}{\varepsilon}\zeta_0(\kappa) z_s} R_g(\omega, \kappa, z_s) S_b(\omega, \boldsymbol{\kappa}) \Big], \end{aligned} \tag{2.18}$$

where R_g and T_g are the coefficients defined by:

$$R_g(\omega, \kappa, z) = \frac{\frac{\overline{\beta}}{\overline{\alpha}}(\omega, \kappa, -L, z)}{\overline{\alpha}(\omega, \kappa, z, 0) + \beta(\omega, \kappa, z, 0)\frac{\overline{\beta}}{\overline{\alpha}}(\omega, \kappa, -L, z)}, \tag{2.19}$$

$$T_g(\omega, \kappa, z) = \frac{1}{\overline{\alpha}(\omega, \kappa, z, 0) + \beta(\omega, \kappa, z, 0)\frac{\overline{\beta}}{\overline{\alpha}}(\omega, \kappa, -L, z)}. \tag{2.20}$$

These coefficients are generalized versions of the coefficients used in [1] as we explain now. The transmission and reflection coefficients $T(\omega, \kappa, -L, z)$ and $R(\omega, \kappa, -L, z)$ for a slab $[-L, z]$ (see Figure 2.2) are given in terms of α and β by

$$R(\omega, \kappa, -L, z) = \frac{\overline{\beta}}{\overline{\alpha}}(\omega, \kappa, -L, z), \qquad T(\omega, \kappa, -L, z) = \frac{1}{\overline{\alpha}}(\omega, \kappa, -L, z).$$

We also introduce $\widetilde{R}$ and $\widetilde{T}$ defined as the reflection and transmission coefficients for the experiment corresponding to a right-going input wave incoming from the left (see Figure 2.3). They are given in terms of α and β by

$$\widetilde{R}(\omega, \kappa, z, 0) = -\frac{\beta}{\overline{\alpha}}(\omega, \kappa, z, 0), \qquad \widetilde{T}(\omega, \kappa, z, 0) = \frac{1}{\overline{\alpha}}(\omega, \kappa, z, 0).$$

We can express the coefficients R_g and T_g in terms of the usual reflection and transmission coefficients for which the asymptotic analysis of the moments has been carried out in [1] and will be used in subsequent sections:

$$R_g(\omega, \kappa, z) = \frac{\widetilde{T}(\omega, \kappa, z, 0) R(\omega, \kappa, -L, z)}{1 - \widetilde{R}(\omega, \kappa, z, 0) R(\omega, \kappa, -L, z)}, \tag{2.21}$$

$$T_g(\omega, \kappa, z) = \frac{\widetilde{T}(\omega, \kappa, z, 0)}{1 - \widetilde{R}(\omega, \kappa, z, 0) R(\omega, \kappa, -L, z)}. \tag{2.22}$$

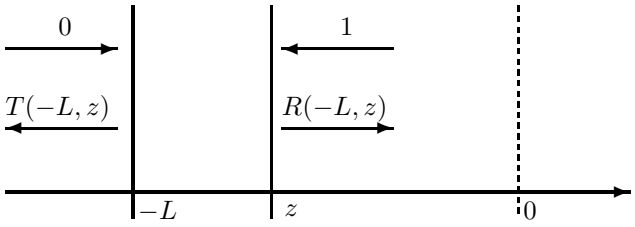

FIG. 2.2. *Reflection and transmission coefficients.*

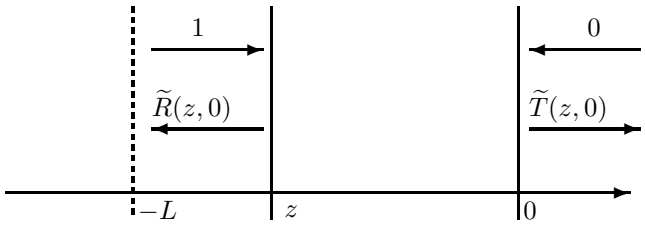

FIG. 2.3. *Adjoint reflection and transmission coefficients.*

We denote the wave at the surface $z = 0$ by $(\mathbf{u}_o, p_o)$. By taking an inverse Fourier transform we finally obtain the integral representations

$$p_o(t,\mathbf{x}) = \frac{1}{(2\pi\varepsilon)^3}\int \frac{\sqrt{I_0(\kappa)}}{2} a(\omega,\boldsymbol{\kappa},0) e^{-i\frac{\omega}{\varepsilon}(t-\boldsymbol{\kappa}\cdot\mathbf{x})}\omega^2 d\omega d\boldsymbol{\kappa}, \tag{2.23}$$

$$u_o(t,\mathbf{x}) = \frac{1}{(2\pi\varepsilon)^3}\int \frac{1}{2\sqrt{I_0(\kappa)}} a(\omega,\boldsymbol{\kappa},0) e^{-i\frac{\omega}{\varepsilon}(t-\boldsymbol{\kappa}\cdot\mathbf{x})}\omega^2 d\omega d\boldsymbol{\kappa}, \tag{2.24}$$

$$\mathbf{v}_o(t,\mathbf{x}) = \frac{1}{(2\pi\varepsilon)^3}\int \frac{\sqrt{I_0(\kappa)}}{2\rho_0} \boldsymbol{\kappa} a(\omega,\boldsymbol{\kappa},0) e^{-i\frac{\omega}{\varepsilon}(t-\boldsymbol{\kappa}\cdot\mathbf{x})}\omega^2 d\omega d\boldsymbol{\kappa}. \tag{2.25}$$

2.2. Emission of a random noise from a point source. In this subsection we revisit the derivation of the integral representation of the wave field in the case where the point source emits a stationary random signal with Gaussian statistics. The spectral representation of the signal is given by (1.8), so that we must adapt the integral representation of the field observed at the surface. If we focus our attention on the pressure field, then we get

$$\begin{aligned} p_o(t,\mathbf{x}) = {} & \frac{1}{(2\pi)^{\frac{5}{2}}\varepsilon^{\frac{3}{2}}}\int T_g(\omega,\kappa,z_s)\vec{\mathbf{S}}_a(\omega,\boldsymbol{\kappa}) e^{i\frac{\omega}{\varepsilon}(-\boldsymbol{\kappa}\cdot\mathbf{x}_s)-i\frac{\omega}{\varepsilon}(t-\boldsymbol{\kappa}\cdot\mathbf{x})-i\frac{\omega}{\varepsilon}\zeta_0(\kappa)z_s}\omega^2 d\boldsymbol{\kappa} d\vec{\mathbf{W}}_\omega \\ & + \frac{1}{(2\pi)^{\frac{5}{2}}\varepsilon^{\frac{3}{2}}}\int R_g(\omega,\kappa,z_s)\vec{\mathbf{S}}_b(\omega,\boldsymbol{\kappa}) e^{i\frac{\omega}{\varepsilon}(-\boldsymbol{\kappa}\cdot\mathbf{x}_s)-i\frac{\omega}{\varepsilon}(t-\boldsymbol{\kappa}\cdot\mathbf{x})+i\frac{\omega}{\varepsilon}\zeta_0(\kappa)z_s}\omega^2 d\boldsymbol{\kappa} d\vec{\mathbf{W}}_\omega, \end{aligned} \tag{2.26}$$

where

$$\vec{\mathbf{S}}_a(\omega,\boldsymbol{\kappa}) = \frac{1}{2}\begin{pmatrix} \frac{I_0(\kappa)}{\rho_0}\boldsymbol{\kappa} \\ 1 \end{pmatrix}\cdot\hat{g}(\omega), \qquad \vec{\mathbf{S}}_b(\omega,\boldsymbol{\kappa}) = \frac{1}{2}\begin{pmatrix} \frac{I_0(\kappa)}{\rho_0}\boldsymbol{\kappa} \\ -1 \end{pmatrix}\cdot\hat{g}(\omega). \tag{2.27}$$

The velocity field $(\mathbf{v}_s, u_s)$ has a similar expression.

3. Source localization in random media: a brief review. Localization of an acoustic source in the ocean or the earth is often limited because of lack of knowledge

of the physical properties of the medium. It is an important issue to determine how medium uncertainties transfer to uncertainties for source localization. It is also a challenge to propose an efficient approach that gives a robust source localization without requiring an exact knowledge of the medium.

The so-called matched field method estimates source range and depth by matching acoustic fields measured at an array of sensors with simulated fields computed for a grid of possible source locations using a numerical propagation model [34, 2]. The source position is estimated as the position of the maximum match. Matched field methods require good knowledge of the physical properties of the environment which strongly affect the propagation of acoustic fields. However, environmental properties are often poorly known and environmental uncertainty usually represents the limiting factor in localization [29, 28]. Several approaches have been developed to address this limitation.

In geoacoustic inversion a survey is carried out in a particular region. The goal is to determine the physical parameters that are appropriate for subsequent localization problems in the area. The inversion of the measured fields from a known source is a strongly nonlinear problem. Huge effort has been applied using global search methods such as simulating annealing [14], genetic algorithms [19], and hybrid inversions [20]. In the case where the medium is poorly known, the method of focalization addresses environmental uncertainty by including the physical parameters of the medium as additional unknowns in an augmented localization problem [12]. Bayesian approaches are often used in such configurations [27, 33]. Our goal in this paper is to propose an efficient procedure for source localization without knowing the medium. It is based on our analysis of the statistical properties of the observed fields.

4. Embedded source emitting a short pulse. In this section we assume that the source term $\vec{\mathbf{f}}^{\varepsilon}(t)$ corresponds to a short pulse. The source is somewhere below the surface ($\mathbf{x}_s, z_s < 0$). We start by considering the case of a homogeneous medium, as we shall study the problem of the source localization and contrast the homogeneous and random configurations.

4.1. Homogeneous medium. We assume in this section that the medium is homogeneous $\nu \equiv 0$. The signal that can be recorded is a spherical wave emitted from the source located in $S = (\mathbf{x}_s, z_s)$. Using the notation $\vec{\mathbf{r}} = (\mathbf{x}, z)$ and applying the far-field approximation $|\vec{\mathbf{r}} - \vec{\mathbf{r}}_s| \gg \varepsilon$ the pressure signal is

$$p^{\hom}(t,\vec{\mathbf{r}}) = \frac{1}{4\pi c_0 \varepsilon |\vec{\mathbf{r}} - \vec{\mathbf{r}}_s|^2} (\vec{\mathbf{r}} - \vec{\mathbf{r}}_s) \cdot \begin{pmatrix} \mathbf{f}'_{\mathbf{x}} \\ f'_z \end{pmatrix} \left(\frac{t - t_s - \frac{|\vec{\mathbf{r}} - \vec{\mathbf{r}}_s|}{c_0}}{\varepsilon} \right), \tag{4.1}$$

while the three-dimensional velocity field is

$$\vec{\mathbf{u}}^{\hom}(t,\vec{\mathbf{r}}) = \frac{\vec{\mathbf{r}} - \vec{\mathbf{r}}_s}{4\pi \rho_0 c_0^2 \varepsilon |\vec{\mathbf{r}} - \vec{\mathbf{r}}_s|^3} (\vec{\mathbf{r}} - \vec{\mathbf{r}}_s) \cdot \begin{pmatrix} \mathbf{f}'_{\mathbf{x}} \\ f'_z \end{pmatrix} \left(\frac{t - t_s - \frac{|\vec{\mathbf{r}} - \vec{\mathbf{r}}_s|}{c_0}}{\varepsilon} \right). \tag{4.2}$$

Application to source localization. Assume that the source location $S = (\mathbf{x}_s, z_s)$ and the source emission time t_s are unknown. Assume that four observation points located in O_j, $j = 1, \cdots, 4$, at the surface record the pressure signals. We are thus able to detect four arrival times

$$T_j = t_s + \frac{1}{c_0} |O_j S|,$$

where $|O_jS|$ is the physical distance between O_j and S. We can thus invert the four arrival times to get the four unknowns $(\mathbf{x}_s, z_s, t_s)$.

4.2. The coherent pulse front in the random case. The signals (2.23-2.25) consist of a coherent front wave of duration of the order of ε corresponding to the duration of the source, and a long noisy coda part that is caused by the multiple scattering by the layers. In this section we compute the expression of the coherent front pulse that can be recorded at the surface. The front pulse emitted by the source propagates through the random medium and its propagation is governed by the well known O'Doherty Anstey (ODA) theory [24]. In Section 4.1 we computed this front pulse in homogeneous medium. We now revisit these results in presence of randomness. In this case the front pulse is modified in two ways. First its shape spreads out in a deterministic way due to multiple scattering. This spreading can be described in terms of the convolution ODA kernel K_{ODA} [10, 21, 4, 18]. Second the wave itself is not anymore deterministic but a random time shift can be observed and described in terms of a standard Brownian motion B_z. To sum-up, the pulse front that can be recorded at the surface $z = 0$ is

$$p_o(t,\mathbf{x}) = \frac{1}{(2\pi)^3\varepsilon^2}\int \frac{\sqrt{I_0(\kappa)}}{2} e^{-i\frac{\omega}{\varepsilon}(t-t_s-\boldsymbol{\kappa}\cdot(\mathbf{x}-\mathbf{x}_s)+\zeta_0(\kappa)z_s)}\hat{K}_{\mathrm{ODA}}(\omega,\boldsymbol{\kappa})S_a(\omega,\boldsymbol{\kappa})\omega^2 d\omega d\boldsymbol{\kappa}$$

where

$$\hat{K}_{\mathrm{ODA}}(\omega,\boldsymbol{\kappa}) = \exp\left(i\sqrt{\gamma(\omega,\kappa)}B_{z_s} + \frac{\gamma(\omega,\kappa)z_s}{2}\right), \tag{4.3}$$

$$\gamma(\omega,\kappa) = \frac{\gamma_0\omega^2}{2c_0^4\zeta_0(\kappa)^2}, \qquad \gamma_0 = \int_0^\infty \mathbb{E}[\nu(0)\nu(z)]dz. \tag{4.4}$$

The rapid phase $-\omega\left(t - t_s - \boldsymbol{\kappa}\cdot(\mathbf{x}-\mathbf{x}_s) + \zeta_0(\kappa)z_s\right)$ is involved in the integral representation of p_o. A stationary phase argument shows that the leading order contribution is associated with the stationary point $\boldsymbol{\kappa} = \frac{\mathbf{x}-\mathbf{x}_s}{\sqrt{|\mathbf{x}-\mathbf{x}_s|^2+z_s^2}}$. In the case $\gamma_0 = 0$, the expression of p_o reduces exactly to (4.2) with $z = 0$. If we denote the pressure in the homogeneous medium by p^{hom}, then in presence of randomness $\gamma_0 > 0$ the pressure field can be written as the convolution with a Gaussian kernel

$$p_o(t,\mathbf{x}) = \left[p^{\mathrm{hom}}(\cdot,\vec{\mathbf{r}}=(\mathbf{x},0)) * \mathcal{N}_{\mathbf{x}}\right]\left(t - \frac{\sqrt{\gamma_{\mathbf{x}}}}{\sqrt{2}c_0}B_{z_s}\right),$$

where

$$\mathcal{N}_{\mathbf{x}}(t) = \frac{c_0}{\sqrt{\gamma_{\mathbf{x}}|z_s|\pi}}\exp\left(-\frac{c_0^2t^2}{\gamma_{\mathbf{x}}|z_s|}\right), \qquad \gamma_{\mathbf{x}} = \gamma_0\frac{|\mathbf{x}-\mathbf{x}_s|^2+z_s^2}{z_s^2}. \tag{4.5}$$

4.3. Application to source localization. We are able to detect the arrival times at each observation point

$$T_j = t_s + \frac{1}{c_0}|O_jS| + \varepsilon\frac{\sqrt{\gamma_{\mathbf{x}_j}}}{\sqrt{2}c_0}B_{z_s}.$$

We aim at inverting these equations to determine the source location. The situation seems more complicated than in the homogeneous case because of the presence of

the random time shifts. However these unknown shifts can be removed. From the expression of $\gamma_{\mathbf{x}}$, we can write

$$T_j = t_s + \frac{1}{c_0}|O_jS|\,(1+Z_s)\,, \qquad Z_s = \varepsilon\frac{\sqrt{\gamma_0}}{\sqrt{2}|z_s|}B_{z_s}. \tag{4.6}$$

The analysis shows that Z_s does not depend on the observation point. We are thus in a position to propose a way to compute the source location that will be error-free if we have five observation points. This procedure consists in inverting the five arrival times to determine the source location $S = (\mathbf{x}_s, z_s)$, the source emission time t_s, and the random delay Z_s. It is described and discussed in the next subsection.

4.4. Numerical simulations. In this subsection we perform numerical simulations of the acoustic equations to check our theoretical predictions. We consider a medium with a constant-stepwise bulk-modulus. This means that the bulk modulus is constant in each elementary layer with width δz. In each layer ν takes a value which is equal to $\pm\sigma_\kappa$ with probability 1/2. The source located in $(\mathbf{0}, z_s)$ emits a signal with duration t_c. The time profile of f_z is the derivative of a Gaussian $t\exp(-t^2/t_c^2)$, its Fourier transform is (up to a multiplicative constant) $\omega\exp(-\omega^2 t_c^2/4)$. The two other components f_x and f_y are zero. The vertical direction of the point source makes the solution radially symmetric. This allows us to use polar coordinates and the one-dimensional Hankel transform instead of the two-dimensional Fourier transform in the transverse directions.

$$\hat{p}(\omega,k,z) = \int_{-\infty}^{\infty}\int_0^{\infty} p(t,r,z)J_0(k\omega r)e^{i\omega t}r\,dr\,dt,$$
$$p(t,r,z) = \frac{1}{(2\pi)^3}\int_{-\infty}^{\infty}\int_0^{\infty} \hat{p}(\omega,k,z)J_0(k\omega r)e^{-i\omega t}\omega^2\,dk\,d\omega.$$

We apply the numerical routine proposed by Asch *et al* [1]. This code was designed to address the difficulties inherent to multiple scales problems. It splits the problem into a family of ordinary differential equations for the right- and left-going modes in the (ω, k) space. It also avoids numerical instabilities due to the multiplication of large exponentials in the transfer matrices. It turns out that the code provides accurate results, so we simply adapt it to our case without fundamental improvement.

The configuration is $z_s = -30$, $t_c = 2$, $L = 50$, $\delta z = 0.1$, $\rho_0 = 1$, $K_0 = 1$, and thus $c_0 = 1$. There is accordingly a stack of 300 layers between the source and the surface. The (ω, k) space is discretized on a grid with size 256×4096. The observation points are $O_1 = (0,0,0)$, $O_2 = (5,0,0)$ $O_3 = (0,-5,0)$, $O_4 = (-10,0,0)$, and $O_5 = (15,0,0)$.

We first test our code in absence of inhomogeneities $\sigma_\kappa = 0$. In Figure 4.1a we plot the recorded signals. All signals have the same shapes and are time-delayed by the travel-times from the source to the observation points. Eq. (4.1) predicts that the profiles of the recorded signals should be the second derivative of a Gaussian $(1-2t^2/t_c^2)\exp(-t^2/t_c^2)$, which is almost the case in the numerical simulations. There is a slight departure (asymmetry) due to the fact that the far-field condition $|SO_j| \ll c_0 t_c$ is only fulfilled with an accuracy of ~ 0.1. We can detect the maxima of the recorded signals. We get $T_1 = 30.02$, $T_2 = 30.42$, $T_3 = 30.42$, $T_3 = 31.64$, and $T_4 = 33.56$, while the theoretical values should be $T_1 = 30$, $T_2 = 30.41$, $T_3 = 30.41$, $T_4 = 31.62$, and $T_5 = 33.54$.

We have also performed numerical simulations with two different realizations of the random medium with $\sigma_\kappa = 0.8$. In Figure 4.2a we compare the signals recorded

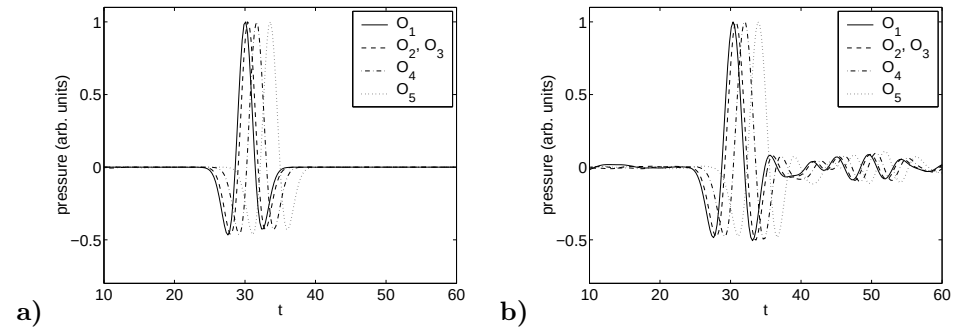

FIG. 4.1. *Signals recorded at the observation points. Picture a: homogeneous medium. Picture b: random medium,* $\sigma_\kappa = 0.8$ *You can observe the resemblance between the two signals up to a time shift.*

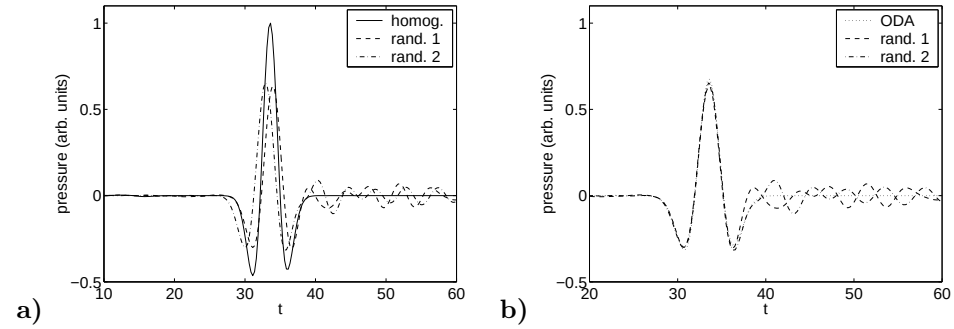

FIG. 4.2. *Signals recorded at the observation point* 0_4. *Picture a: comparisons between the signal obtained from a homogeneous medium and the signals obtained from simulations with two different realizations of the random medium,* $\sigma_\kappa = 0.8$. *Picture b: Comparisons between the theoretical front pulse obtained by the ODA theory and the signals obtained from simulations (and time-shifted by the user to remove the random time shifts). The front pulse can be seen to be perfectly predicted.*

at the same observation point 0_4, in absence of randomness, and with two different realizations of the random medium. The recorded signals in presence of randomness contain a short coherent front signal and a small-amplitude long coda. We can thus check the ODA theory as the shapes of the recorded signals are obviously deterministic in that they do not depend on the particular realization of the medium, while the coda is changing when the medium is changed. We can even check the ODA theory quantitatively. In Figure 4.2b we take the signal corresponding to the homogeneous case, convolute it with the deterministic ODA kernel (4.5), and compare the convoluted signal with the random recorded signals time-shifted to allow better comparison. The agreement is indeed excellent. Finally, in Figure 4.1b we plot the signals recorded at all observation points for the first realization of the medium. We can detect the maxima of the recorded signals. We get $T_1 = 30.36$, $T_2 = 30.78$, $T_3 = 30.78$, $T_3 = 32.0$, and $T_4 = 33.94$.

We would like now to invert the data (the arrival times of the pulse fronts) in order to get the source location and emission time. We first apply the usual deterministic localization procedure with the five observation points. We minimize the matching

function

$$f(\mathbf{x},z,t)=\sum_{j=1}^{5}\left|\sqrt{|\mathbf{x}-\mathbf{x}_j|^2+z^2}-c_0(T_j-t)\right|^2$$

over $\mathbf{x}\in\mathbb{R}^2$, $z\in\mathbb{R}^-$, and $t\in\mathbb{R}$. The minimum is reached at $(\hat{\mathbf{x}}_s,\hat{z}_s,\hat{t}_s)$ where $(\hat{\mathbf{x}}_s,\hat{z}_s)$ is the estimated source location and $\hat{t}_s$ is the estimated source emission time. In the homogeneous case $\sigma_\kappa=0$, we have got $\hat{\mathbf{x}}_s=(0,0)$, $\hat{z}_s=-29.95$, and $\hat{t}_s=0.05$. We can observe a small error with respect to the true position which is compatible with the numerical accuracy of our simulations. In the random case we have got $\hat{\mathbf{x}}_s=(0,0)$, $\hat{z}_s=-29.65$, and $t_s=0.7$. We can now observe an error of about 0.5 with respect to the true position which is expected, because in this case $\gamma_0=0.019$ and $\mathrm{Var}(T_j)=\gamma_0|O_jS|^2/(2|z_s|)\sim\gamma_0|z_s|/2\sim 0.5$.

Let us now apply an alternative localization procedure taking into account the random delay. The matching function is

$$f(\mathbf{x},z,t,\eta)=\big(1+\alpha\eta^2\big)\sum_{j=1}^{5}\left|\sqrt{|\mathbf{x}-\mathbf{x}_j|^2+z^2}(1+\eta)-c_0(T_j-t)\right|^2,$$

with $\mathbf{x}\in\mathbb{R}^2$, $z\in\mathbb{R}^-$, $t\in\mathbb{R}$, and $\eta\in(-1,1)$. The parameter η models the random delay according to the asymptotic form (4.6). The regularizing factor $1+\alpha\eta^2$ ensures that the optimization effort is put onto the source localization and not on the random delay. The parameter α should be chosen by the user, but it can also be helpful to have a guess of the magnitude of Z_s. In our case we expect $|Z_s|\sim 0.02$ so we have chosen $\alpha=1000$ but the exact value is not critical. In the homogeneous case we get the same estimated point as the one obtained with the first procedure. In the random case, with the same data as the ones used for the application of the first procedure, we have got $\hat{\mathbf{x}}_s=(0,0)$, $\hat{z}_s=-30.1$, and $\hat{t}_s=-0.1$ which is better than the estimates obtained with the first procedure in the random case, and of the same accuracy as the result obtained in the homogeneous case.

5. Embedded source emitting a stationary random signal. In this section we assume that the source term $\vec{\mathbf{f}}^{\varepsilon}(t)$ is a stationary random noise. In such conditions no front pulse can be detected, as the recorded signals are themselves stationary. However we shall see that the cross-correlation function between the signals recorded at two observation points gives useful information, in the sense that 1) it depends on the position of the source and 2) it is statistically stable with respect to the statistical distribution of the medium and with respect to the statistical distribution of the noise emitted by the source.

5.1. The cross-correlation function. We assume that we record the pressure field at two observation points $\mathbf{x}_1$ and $\mathbf{x}_2$ during some time window. We compute the cross-correlation function (CCF)

$$C(t_0+\varepsilon\sigma)=\int_{-\infty}^{\infty}p_o(t,\mathbf{x}_1)p_o(t+t_0+\varepsilon\sigma,\mathbf{x}_2)G(t)dt, \tag{5.1}$$

where G stands for the time window function. For instance, we may think at $G(t)=\mathbf{1}_{[0,T_0]}(t)$ but we only need G to belong to $L^1\cap L^2$. Considering the integral representation (2.26) of p_o, we observe that the CCF can be written as the sum of four

integrals, with crossed terms $T_g\overline{T_g}$, $T_g\overline{R_g}$, $R_g\overline{T_g}$, and $R_g\overline{R_g}$, respectively. Let us consider the first one and take the expectation with respect to the distribution of the source signal. We get

$$\langle C_I\rangle(t_0+\varepsilon\sigma) = \frac{1}{(2\pi)^5\varepsilon^3}\int D(\omega,\boldsymbol{\kappa},\boldsymbol{\kappa}')T_g(\omega,\kappa',z_s)\overline{T_g}(\omega,\kappa,z_s)e^{i\omega\sigma}e^{i\frac{\omega}{\varepsilon}t_0}$$
$$\times e^{i\frac{\omega}{\varepsilon}(\boldsymbol{\kappa}-\boldsymbol{\kappa}')\cdot\mathbf{x}_s+i\frac{\omega}{\varepsilon}(\boldsymbol{\kappa}'\cdot\mathbf{x}_1-\boldsymbol{\kappa}\cdot\mathbf{x}_2)+i\frac{\omega}{\varepsilon}(\zeta_0(\kappa)-\zeta_0(\kappa'))z_s}\omega^4 d\boldsymbol{\kappa}' d\boldsymbol{\kappa} d\omega, \tag{5.2}$$

where

$$D(\omega,\boldsymbol{\kappa},\boldsymbol{\kappa}') = \frac{1}{4}\begin{pmatrix}\frac{I_0(\kappa)}{\rho_0}\boldsymbol{\kappa}\\ 1\end{pmatrix}\cdot\hat{\mathcal{G}}(\omega)\begin{pmatrix}\frac{I_0(\kappa')}{\rho_0}\boldsymbol{\kappa}'\\ 1\end{pmatrix}\times\int_{-\infty}^{\infty}G(t)dt. \tag{5.3}$$

5.2. The stationary phase. In the integral representation (5.2) we use polar coordinates (μ,θ) and (μ',θ') for $\boldsymbol{\kappa}=\mu\mathbf{e}_\theta$ and $\boldsymbol{\kappa}'=\mu'\mathbf{e}_{\theta'}$, where we denote by $\mathbf{e}_\theta$ the unit column vector $(\cos(\theta),\sin(\theta))^T$. We also parameterize the observation points $\mathbf{x}_1$ and $\mathbf{x}_2$ relatively to the source offset: $\mathbf{x}_1=\mathbf{x}_s+r_1\mathbf{e}_{\theta_1}$, $\mathbf{x}_1=\mathbf{x}_s+r_2\mathbf{e}_{\theta_2}$. We get

$$\langle C_I\rangle(t_0+\varepsilon\sigma) = \frac{1}{(2\pi)^5\varepsilon^3}\int \tilde{D}(\omega,\mu,\mu',\theta,\theta')T_g(\omega,\mu',z_s)\overline{T_g}(\omega,\mu,z_s)e^{i\omega\sigma}$$
$$\times e^{i\frac{\omega}{\varepsilon}\left[r_1\mu'\cos(\theta'-\theta_1)-r_2\mu\cos(\theta-\theta_2)+(\zeta_0(\mu)-\zeta_0(\mu'))z_s+t_0\right]}\omega^4\mu'\mu d\theta d\theta' d\mu' d\mu d\omega, \tag{5.4}$$

where $\tilde{D}(\omega,\mu,\mu',\theta,\theta') = D(\omega,\mu\mathbf{e}_\theta,\mu'\mathbf{e}_{\theta'})$. We apply a stationary phase argument. We find that there exists a stationary map given by

$$\mu_c' = \frac{1}{c_0}\frac{r_1}{\sqrt{r_1^2+z_s^2}},\qquad \mu_c = \frac{1}{c_0}\frac{r_2}{\sqrt{r_2^2+z_s^2}},\qquad \theta_c'=\theta_1,\qquad \theta_c=\theta_2,$$

only if $t_0 - r_2\mu_c + z_s\zeta_0(\mu_c) + r_1\mu_c' - z_s\zeta_0(\mu_c') = 0$, which also reads as $t_0 = t_c$ with

$$t_c = \frac{1}{c_0}\left(\sqrt{r_2^2+z_s^2}-\sqrt{r_1^2+z_s^2}\right). \tag{5.5}$$

We then find that, to leading order in ε,

$$\langle C_I\rangle(t_c+\varepsilon\sigma) = \int D_I(\omega)T_g(\omega,\mu_c',z_s)\overline{T_g}(\omega,\mu_c,z_s)e^{i\omega\sigma}\omega^2 d\omega,$$

where

$$D_I(\omega) = \frac{1}{(2\pi)^2}\frac{1}{c_0^2}\frac{|z_s|^3}{(r_1^2+z_s^2)(r_2^2+z_s^2)}\tilde{D}(\omega,\mu_c,\mu_c',\theta_c,\theta_c'). \tag{5.6}$$

depends only on ω, $\mathbf{x}_1$, $\mathbf{x}_2$, and $(\mathbf{x}_s,z_s)$. We get similar expressions for the three other components of $\langle C\rangle$ which depend on the products $T_g\overline{R_g}$, $R_g\overline{T_g}$, and $R_g\overline{R_g}$.

5.3. Statistical distribution with respect to the medium.

5.3.1. Tightness. We first address the tightness of the process.

LEMMA 5.1. *For any $t_0\in\mathbb{R}$, the process $(\langle C_I\rangle(t_0+\varepsilon\sigma))_{-\infty<\sigma<\infty})_{\varepsilon>0}$ is a tight (i.e. weakly compact) family in the space of continuous trajectories.*

Proof. We must show that, for any $\delta>0$, there exists a compact subset K of the space of continuous bounded functions such that:

$$\sup_{\varepsilon>0}\mathbb{P}(\langle C_I\rangle(t_0+\varepsilon\cdot)\in K)\geq 1-\delta.$$

On the one hand the generalized transmission coefficient can also be rewritten as $T_g = \overline{\alpha}(-L,z_s)/\overline{\alpha}(-L,0) = T(-L,0)/T(-L,z_s)$ which shows that $|T_g| \leq 1$ so $\langle C_I \rangle (t_0+\varepsilon t)$ is uniformly bounded by:

$$|\langle C_I \rangle (t_0+\varepsilon\sigma)| \leq \int |D_I(\omega)| d\omega. \tag{5.7}$$

The right-hand side is a finite quantity because $|D_I(\omega)| \leq K|\hat{\mathcal{G}}(\omega)|$ where K depends only on $\mathbf{x}_1$, $\mathbf{x}_2$, and $(\mathbf{x}_s, z_s)$ and $\omega \mapsto \omega^2|\hat{\mathcal{G}}|(\omega)$ is in L^1 by assumption. On the other hand the modulus of continuity

$$M^\varepsilon(\delta) = \sup_{|\sigma_1-\sigma_2|\leq\delta} |\langle C_I \rangle (t_0+\varepsilon\sigma_1) - \langle C_I \rangle (t_0+\varepsilon\sigma_2)|$$

is bounded by

$$M^\varepsilon(\delta) \leq \int \sup_{|\sigma_1-\sigma_2|\leq\delta} |1-\exp(i\omega(s_1-s_2))||D_I(\omega)|d\omega,$$

which goes to zero as δ goes to zero uniformly with respect to ε. □

5.3.2. Convergence of the finite-dimensional distributions. The uniform boundedness (5.7) implies that the finite-dimensional distributions of the process $\langle C_I \rangle (t_0+\varepsilon\cdot)$ will be characterized by the moments

$$\mathbb{E}[\langle C_I \rangle (t_0+\varepsilon\sigma_1)^{p_1} \ldots \langle C_I \rangle (t_0+\varepsilon\sigma_k)^{p_k}] \tag{5.8}$$

for every real numbers $\sigma_1 < \ldots < \sigma_k$ and every integers $p_1, \ldots, p_k$. We have seen that $\langle C_I(t_0+\varepsilon\sigma)\rangle$ is at most of order $\sqrt{\varepsilon}$ if $t_0 \neq t_c$, so that its moments are vanishing. We accordingly address the relevant case $t_0 = t_c$.

First moment. The computation of the expectation of $\langle C_I(t_c+\varepsilon\sigma)\rangle$ is reduced to the computation of the expectation of

$$U_g^\varepsilon(\omega) = \overline{T_g}(\omega,\mu_c,z_s)T_g(\omega,\mu_c',z_s).$$

Using the representation (2.22) of the generalized coefficient T_g in terms of the usual reflection and transmission coefficients, we obtain the series expansion

$$U_g^\varepsilon(\omega) = \sum_{n,m=0}^{\infty} \overline{R}^n \; R^m \; \widetilde{R}^n \widetilde{T} \; \overline{\widetilde{R}}^m \overline{\widetilde{T}},$$

where $\overline{R}^n$ is evaluated at $(\omega,\mu_c,-L,z_s)$, R^m is evaluated at $(\omega,\mu_c',-L,z_s)$, $\widetilde{R}^n\widetilde{T}$ is evaluated at $(\omega,\mu_c',z_s,0)$, and $\overline{\widetilde{R}}^n\overline{\widetilde{T}}$ is evaluated at $(\omega,\mu_c,z_s,0)$. As $\varepsilon\to 0$ the propagators between $-L$ and z_s and between z_s and 0 become independent. Accordingly we shall obtain the limit of $\mathbb{E}[U_g^\varepsilon(\omega)]$ as $\varepsilon\to 0$ by looking at the limits of $\mathbb{E}[\overline{R}^n R^m]$ and $\mathbb{E}[\widetilde{R}^n\widetilde{T}\overline{\widetilde{R}}^m\overline{\widetilde{T}}]$. Two cases should be distinguished.

1) If $\mu_c \neq \mu_c'$. Let us consider the moment $\mathbb{E}[\overline{R}^n(\omega,\mu_c,-L,z_s)R^m(\omega,\mu_c',-L,z_s)]$. As $\mu_c \neq \mu_c'$, it goes to zero if $(n,m) \neq (0,0)$ (see Appendix A.1). Accordingly the limit of the expectation of $U_g^\varepsilon(\omega)$ is equal to the limit of $\mathbb{E}[\widetilde{T}(\omega,\mu_c',z_s,0)\overline{\widetilde{T}}(\omega,\mu_c,z_s,0)]$. This limit is computed in Appendix A.1 and we get

$$\mathbb{E}[U_g^\varepsilon(\omega)] \overset{\varepsilon\to 0}{\longrightarrow} \mathbb{E}\left[T_{\text{eff}}(\omega,\mu_c',z_s)\overline{T_{\text{eff}}}(\omega,\mu_c,z_s)\right],$$

where

$$T_{\text{eff}}(\omega,\mu,z_s)=\exp\left(i\sqrt{\gamma(\omega,\mu)}B_{z_s}+\frac{\gamma(\omega,\mu)}{2}z_s\right), \tag{5.9}$$

γ is defined by (4.4), and B is a standard one-dimensional Brownian motion.

2) If $\mu_c=\mu_c'$. By using the expressions of the limit values for moments of reflection and transmission coefficients obtained in Appendix A.2, we get that

$$\mathbb{E}\left[R^n\overline{R}^m\right]\overset{\varepsilon\to0}{\longrightarrow}\begin{cases}0 & \text{if } m\neq n,\\ W_n(\omega,\mu_c,-L,z_s) & \text{if } m=n,\end{cases}$$
$$\mathbb{E}\left[\widetilde{R}^n\widetilde{T}\,\overline{\widetilde{R}}^m\overline{\widetilde{T}}\right]\overset{\varepsilon\to0}{\longrightarrow}\begin{cases}0 & \text{if } m\neq n,\\ \widetilde{W}_n(\omega,\mu_c,z_s,0) & \text{if } m=n,\end{cases}$$

where W_n and $\widetilde{W}_n$ are described in Appendix A.2. We can then deduce that

$$\mathbb{E}[U_g^\varepsilon(\omega)]\overset{\varepsilon\to0}{\longrightarrow}W_{g,1}(\omega,\mu_c,z_s),$$

where

$$W_{g,1}(\omega,\mu,z_s)=\sum_{n=0}^{\infty}W_n(\omega,\mu,-L,z_s)\widetilde{W}_n(\omega,\mu,z_s,0). \tag{5.10}$$

In the following we shall neglect this configuration. Indeed it is shown in [1] that the reflection or transmission coefficients at two nearby slowness vectors are correlated only if the moduli of these slowness vectors are close to each other at order ε. Accordingly the configuration $\mu_c=\mu_c'$ happens only if $\mu_c=\mu_c'$ with an accuracy of order ε, which means that $|O_1S|\simeq|O_2S|$ with an accuracy of the order of the wavelength. Such a case is so improbable that we can safely neglect it in practical configurations.

Higher-order moments. Let us now consider the general moment (5.8). Using the representation (5.6) for each factor $\langle C_I\rangle(t_c+\varepsilon\sigma_j)$, these moments can be written as multiple integrals over $p=\sum_{j=1}^k p_j$ frequencies:

$$\mathbb{E}\left[\langle C_I\rangle(t_c+\varepsilon\sigma_1)^{p_1}\dots\langle C_I\rangle(t_c+\varepsilon\sigma_k)^{p_k}\right]=$$
$$\int\dots\int\mathbb{E}\left[\prod_{\substack{1\le j\le k\\ 1\le l\le p_j}}U_g^\varepsilon(\omega_{j,l})\right]\prod_{\substack{1\le j\le k\\ 1\le l\le p_j}}D_I(\omega_{j,l})e^{i\omega_{j,l}\sigma_j}\omega_{j,l}^2d\omega_{j,l}.$$

If we consider a set of n different frequencies $\omega_1,\cdots,\omega_n$, then we get

$$\mathbb{E}\left[\prod_{j=1}^n U_g^\varepsilon(\omega_j)\right]\overset{\varepsilon\to0}{\longrightarrow}\mathbb{E}\left[\prod_{j=1}^n T_{\text{eff}}(\omega_j,\mu_c',z_s)\overline{T_{\text{eff}}}(\omega_j,\mu_c,z_s)\right],$$

where T_{eff} is defined by (5.9). This shows the convergence of the finite-dimensional distributions of $(\langle C_I\rangle(t_c+\varepsilon\sigma))_{-\infty<\sigma<\infty}$ to the ones of the random function

$$\int D_I(\omega)T_{\text{eff}}(\omega,\mu_c',z_s)\overline{T_{\text{eff}}}(\omega,\mu_c,z_s)e^{i\omega\sigma}\omega^2d\omega.$$

5.3.3. Convergence of the distribution. We have just established that the process $\langle C_I \rangle (t_0 + \varepsilon \cdot)$ is tight and that its finite-dimensional distributions converge. We have thus proved the following proposition

PROPOSITION 5.2. *The process $\langle C_I \rangle (t_0+\varepsilon\cdot)$ converges in distribution in the space of the continuous functions as $\varepsilon \to 0$ to 0 if $t_0 \neq t_c$. If $t_0 = t_c$, it converges to*

$$\langle C_I \rangle (t_c + \varepsilon\sigma) \overset{\varepsilon\to 0}{\longrightarrow} \tag{5.11}$$
$$\int D_I(\omega) e^{i\omega\sigma} \exp\left[i\left(\sqrt{\gamma(\omega,\mu_c')} - \sqrt{\gamma(\omega,\mu_c)} \right) B_{z_s} + \frac{\gamma(\omega,\mu_c') + \gamma(\omega,\mu_c)}{2} z_s \right] \omega^2 d\omega.$$

Proceeding similarly for the three other components of $\langle C \rangle$ which depend on the products $T_g\overline{R_g}$, $R_g\overline{T_g}$, and $R_g\overline{R_g}$, we get that these three components are vanishing in the asymptotic framework $\varepsilon \to 0$.

5.4. Statistical stability with respect to the source signal. We consider in this section the second moment of the CCF, where the expectation is taken with respect to the statistical distribution of the stationary source. Using the representation (2.26) we get that

$$\begin{aligned}\left\langle C_I(t_0+\varepsilon\sigma)^2 \right\rangle =& \langle C_I(t_0+\varepsilon\sigma)\rangle^2 \\ &+ \frac{1}{(2\pi)^{10}\varepsilon^6} \int\cdots\int D(\omega_1,\boldsymbol{\kappa}_1,\boldsymbol{\kappa}_4) D(\omega_2,\boldsymbol{\kappa}_2,\boldsymbol{\kappa}_3) |\hat{G}(\frac{\omega_1-\omega_2}{\varepsilon})|^2 \\ &\times e^{i\frac{\omega_1}{\varepsilon}[(\boldsymbol{\kappa}_4-\boldsymbol{\kappa}_1)\cdot\mathbf{x}_s + \boldsymbol{\kappa}_1\cdot\mathbf{x}_1 - \boldsymbol{\kappa}_4\cdot\mathbf{x}_2 + (\zeta_0(\kappa_4)-\zeta_0(\kappa_1))z_s]} e^{i\frac{\omega_1}{\varepsilon}(t_0+\varepsilon\sigma)} \\ &\times e^{i\frac{\omega_2}{\varepsilon}[(\boldsymbol{\kappa}_2-\boldsymbol{\kappa}_3)\cdot\mathbf{x}_s + \boldsymbol{\kappa}_3\cdot\mathbf{x}_1 - \boldsymbol{\kappa}_2\cdot\mathbf{x}_2 + (\zeta_0(\kappa_2)-\zeta_0(\kappa_3))z_s]} e^{i\frac{\omega_2}{\varepsilon}(t_0+\varepsilon\sigma)} \\ \times T_g(\omega_1,\kappa_1,z_s)\overline{T_g}(\omega_1,\kappa_4,z_s) & T_g(\omega_2,\kappa_2,z_s)\overline{T_g}(\omega_2,\kappa_3,z_s) \omega_1^4\omega_2^4 d\boldsymbol{\kappa}_1 d\boldsymbol{\kappa}_2 d\boldsymbol{\kappa}_3 d\boldsymbol{\kappa}_4 d\omega_1 d\omega_2.\end{aligned}$$

Applying a stationary phase argument, the most important contribution arises once again when t_0 is equal to t_c given by Eq. (5.5), and it is equal to

$$\begin{aligned}\left\langle C_I(t_c+\varepsilon\sigma)^2 \right\rangle &= \langle C_I(t_c+\varepsilon\sigma)\rangle^2 + \int\int D_I(\omega_1) D_I(\omega_2) |\hat{G}(\frac{\omega_1-\omega_2}{\varepsilon})|^2 \\ \times T_g(\omega_1,\mu_c',z_s)\overline{T_g}(\omega_1,\mu_c,z_s) & T_g(\omega_2,\mu_c,z_s)\overline{T_g}(\omega_2,\mu_c',z_s) \omega_1^2\omega_2^2 d\omega_1 d\omega_2.\end{aligned}$$

A straightforward estimate shows that the second term is of order ε because the integral over $(\omega_1,\omega_2) \in \mathbb{R}^2$ actually reduces to a narrow diagonal band of width ε due to the $|\hat{G}(\frac{\omega_1-\omega_2}{\varepsilon})|^2$. This holds true as soon as G belongs to L^2, which is the case. Accordingly, we have shown the following proposition.

PROPOSITION 5.3. *The CCF is a self-averaging quantity with respect to the statistical distribution of the stationary source signal. More exactly,*

$$\left\langle C_I(t_0+\varepsilon\sigma)^2 \right\rangle - \langle C_I(t_0+\varepsilon\sigma)\rangle^2 \overset{\varepsilon\to 0}{\longrightarrow} 0.$$

5.5. Statement of the result. We can now state the main result of this section.

PROPOSITION 5.4. *Let t_c be equal to (5.5). If $t_0 \neq t_c$, then the CCF $C(t_0+\varepsilon\cdot)$ converges to 0. If $t_0 = t_c$, then the CCF $C(t_c+\varepsilon\cdot)$ converges in distribution to a random function*

$$C(t_c+\varepsilon\sigma) \overset{\varepsilon\to 0}{\longrightarrow} \int D_I(\omega) \tag{5.12}$$
$$\times \exp\left[i\omega\left(\frac{1}{c_0}\frac{\sqrt{\gamma_0}}{\sqrt{2}} \frac{|O_1S| - |O_2S|}{|z_s|} B_{z_s} + \sigma \right) - \omega^2 \left(\frac{\gamma_0}{4c_0^2} \frac{|O_1S|^2 + |O_2S|^2}{|z_s|} \right) \right] \omega^2 d\omega,$$

where

$$D_I(\omega) = \frac{1}{(4\pi c_0)^2} \frac{|z_s|}{|O_1S|^2|O_2S|^2} \left(\vec{O_1S} \cdot \hat{\mathcal{G}}(\omega) \vec{O_2S} \right) \times \int_{-\infty}^{\infty} G(t)dt,$$

and B is a standard Brownian motion that is independent of the observation points.

In other words the CCF has a deterministic shape which is the inverse Fourier transform of

$$\frac{1}{(4\pi c_0)^2} \frac{|z_s|}{|O_1S|^2|O_2S|^2} \left(\vec{O_1S} \cdot \hat{\mathcal{G}}(\omega) \vec{O_2S} \right) \exp\left(-\frac{\omega^2 T_c^2}{2} \right) \omega^2$$

where

$$T_c^2 = \frac{\gamma_0}{2c_0^2} \frac{|O_1S|^2 + |O_2S|^2}{|z_s|}$$

It is accordingly the convolution of the autocorrelation function of the source signal with a deterministic kernel. In the case where the source signal is a white noise, i.e. the power spectral density matrix is constant $\hat{\mathcal{G}}(\omega) = \hat{\mathcal{G}}_0$, the shape of the CCF is

$$\frac{1}{4(2\pi)^{3/2} c_0^2 T_c^5} \frac{|z_s|}{|O_1S|^2|O_2S|^2} \left(\vec{O_1S} \cdot \hat{\mathcal{G}}_0 \vec{O_2S} \right) (\sigma^2 - T_c^2) \exp\left(-\frac{\sigma^2}{2T_c^2} \right)$$

The CCF has also a random center. The maximum of the CCF $t \mapsto C(t)$ is reached at

$$T_{21} = \frac{1}{c_0} \left(|O_2S| - |O_1S| \right) \left(1 + \varepsilon \frac{\sqrt{\gamma_0}}{\sqrt{2}} \frac{1}{|z_s|} B_{z_s} \right) \tag{5.13}$$

which is a random time depending on the particular realization of the medium.

5.6. Application to source localization. Assume that we have five observation points O_j, $j = 1, \cdots, 5$. Our first aim is to compute the source location. From the recorded signal we are able to detect the maxima of the CCF between O_j, $j = 1, \cdots, 4$ and O_5

$$T_{j5} = \frac{1}{c_0} \left(|O_jS| - |O_5S| \right) (1 + Z_s), \tag{5.14}$$

where $Z_s = \varepsilon \sqrt{\gamma_0/2} B_{z_s}/|z_s|$. The analysis has shown that Z_s does not depend on the observation points. We can propose a way to compute the source location $S = (\mathbf{x}_s, z_s)$ as well as the random delay Z_s that is error-free. The four unknowns satisfy the four independent relations (5.14) and can thus be inverted from the observed times T_j.

Note that the maxima of the CCF give the position of the source. The deterministic shape of the CCF gives the autocorrelation matrix $\hat{\mathcal{G}}$ of the source. Indeed, once the source location is known, by a Fourier transform of the CCF we can get for any frequency ω the value of $\vec{O_jS} \cdot \hat{\mathcal{G}}(\omega) \vec{O_lS}$, $j, l = 1, \cdots, 5$.

5.7. Numerical simulations. In this subsection we perform full numerical simulations to check our theoretical predictions. We consider the same medium as in Subsection 4.4. The only difference is that the source emits a stationary random signal with Gaussian statistics and power spectral density $\omega^2 \exp(-2\omega^2)$.

In Figure 5.1a we plot pieces of the signals recorded at the points O_2 and O_5. Of course there is no front pulse as the source and the recorded signals are stationary

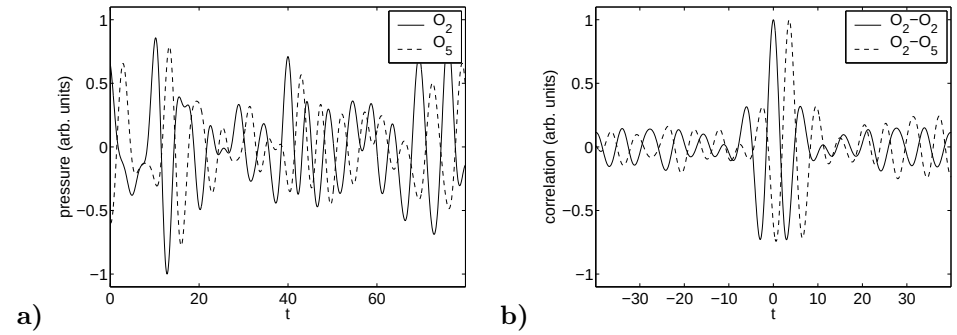

FIG. 5.1. *Picture a: Pieces of the signals recorded at the observation points O_2 and O_5. Picture b: CCFs between the recorded signals.*

random signals. In Figure 5.1b we plot the autocorrelation function of the signal recorded at O_2, as well as the CCF of the two signals recorded at O_2 and O_5. We can detect the maxima of the CCFs. We get $T_{12} = 0.42$, $T_{13} = 0.42$, $T_{14} = 1.64$, $T_{15} = 3.56$, $T_{23} = 0$, $T_{24} = 1.22$, $T_{25} = 3.12$, $T_{34} = 1.22$, $T_{35} = 3.12$, and $T_{45} = 1.90$.

If we apply the basic localization procedure considering the matching function

$$f(\mathbf{x}, z) = \sum_{j=1}^{4} \left| \left(\sqrt{|\mathbf{x} - \mathbf{x}_j|^2 + z^2} - \sqrt{|\mathbf{x} - \mathbf{x}_5|^2 + z^2} \right) - c_0 T_{j5} \right|^2 ,$$

then we get $\hat{\mathbf{x}}_s = (-0.1, 0)$ and $\hat{z}_s = -29.45$ (remember the true location is $\mathbf{x}_s = 0$ and $z_s = -30$). We next apply our localization procedure taking into account the random delay. We consider the matching function

$$f(\mathbf{x}, z, \eta) = \left(1 + \alpha\eta^2\right) \sum_{j=1}^{4} \left| \left(\sqrt{|\mathbf{x} - \mathbf{x}_j|^2 + z^2} - \sqrt{|\mathbf{x} - \mathbf{x}_5|^2 + z^2} \right) (1 + \eta) - c_0 T_{j5} \right|^2 .$$

By minimizing f we get $\hat{\mathbf{x}}_s = 0$ and $\hat{z}_s = -29.98$. The accuracy turns out to be as good as in the case of a source emitting a short pulse. Note that this series of simulations has a large computational cost. Indeed, we face a difficult situation from the numerical point of view. First we need a high precision in the locations of the maxima of the CCF, which requires a fine sampling of the recorded signals with a very small grid step δt, smaller than the coherence time t_c of the source. Second we need a long time window of duration T_0, larger than the coherence time t_c of the source. This long time window insures an efficient ergodic averaging with respect to the statistical distribution of the source which is necessary for an accurate estimate of the CCF (Proposition 5.3). We have taken $T_0 = 2000$ and $\delta t = 0.05$ (remember the coherence time is about 4). With this value of T_0 we are able to detect the maximum of the CCF which is well above the noise level (see Figure 4.2b). With this value of δt, we are able to locate the maximum of the CCF with a precision of about $\delta t/2$. Note that these two problems are specific to the numerical simulations which should resolve three different time scales (the sampling step, the coherence time of the source, and the recording time window) as well as three different spatial scales (the correlation length of the medium, the typical wavelength of the source, and the typical depth of the source). They are not real problems in practical configurations addressing physical signals. So we may consider that we have proved the efficiency of our localization procedure.

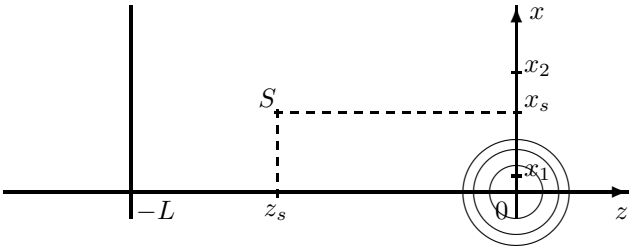

FIG. 6.1. *Emission from a point source located at* $O = (\mathbf{0}, 0)$. *The scatterer position is* $S = (\mathbf{x}_s, z_s)$. *The signal is recorded at different observation points* $O_1 = (\mathbf{x}_1, 0)$, $O_2 = (\mathbf{x}_2, 0)$,....

6. Embedded scatterer illuminated by external sources. The analysis carried out in the previous sections can be extended to the imaging of passive scatterers embedded in a random half-space and illuminated by a source or a set of sources.

6.1. Illumination by a source emitting a short pulse. A source located at the surface at $(\mathbf{0}, 0)$ emits a short pulse at time 0 of the form

$$\vec{\mathbf{f}}^{\varepsilon}(t) = \begin{pmatrix} \mathbf{0} \\ 1 \end{pmatrix} f(\frac{t}{\varepsilon}).$$

In absence of scatterer, the pressure field at the surface is

$$p_0(t, \mathbf{x}) = \frac{1}{(2\pi)^3 \varepsilon^2} \int \frac{1 - R(\omega, \kappa, -L, 0)}{2} e^{-i\frac{\omega}{\varepsilon}(t - \boldsymbol{\kappa}\cdot\mathbf{x})} \hat{f}(\omega)\omega^2 d\omega d\boldsymbol{\kappa}. \tag{6.1}$$

Applying the same methodology as in Section 4, we get the following proposition.

PROPOSITION 6.1. *Let* $t_0 \in \mathbb{R}$ *and* O_1 *be an observation point at the surface. The signal detected at* O_1 *converges in probability as*

$$p(t_0 + \varepsilon\sigma) \stackrel{\varepsilon\to 0}{\longrightarrow} 0, \tag{6.2}$$

$$\mathbf{v}(t_0 + \varepsilon\sigma) \stackrel{\varepsilon\to 0}{\longrightarrow} 0, \tag{6.3}$$

$$u(t_0 + \varepsilon\sigma) \stackrel{\varepsilon\to 0}{\longrightarrow} \begin{cases} -\dfrac{1}{4\pi\rho_0 c_0 |OO_1|^2} f(\sigma) & \text{if } c_0 t_0 = |OO_1|, \\ 0 & \text{otherwise.} \end{cases} \tag{6.4}$$

Similarly, the pressure field at the position $(\mathbf{x}_s, z_s)$ inside the medium ($z_s < 0$) is

$$p_0(t, \mathbf{x}_s, z_s) = \frac{1}{(2\pi)^3 \varepsilon^2} \int \Bigg[\frac{R_g(\omega, \kappa, z_s)}{2} e^{-i\frac{\omega}{\varepsilon}(t - \boldsymbol{\kappa}\cdot\mathbf{x}_s - \zeta_0(\kappa) z_s)} - \frac{T_g(\omega, \kappa, z_s)}{2} e^{-i\frac{\omega}{\varepsilon}(t - \boldsymbol{\kappa}\cdot\mathbf{x}_s + \zeta_0(\kappa) z_s)} \Bigg] \hat{f}(\omega)\omega^2 d\omega d\boldsymbol{\kappa}. \tag{6.5}$$

We now consider a scatterer embedded at $S = (\mathbf{x}_s, z_s)$ (see Figure 6.1). We model this scatterer as a local change in the density of the medium

$$\rho(\mathbf{x}, z) = \rho_0 + \rho_1 \mathbf{1}_B(\mathbf{x}, z),$$

where B is a small domain around S. The system that governs the propagation of the acoustic waves is

$$\rho_0 \frac{\partial \vec{\mathbf{u}}}{\partial t} + \nabla p = \mathbf{f}^{\varepsilon}(t)\delta(\mathbf{x})\delta(z) - \rho_1 \mathbf{1}_B(\mathbf{x}, z) \frac{\partial \vec{\mathbf{u}}}{\partial t}, \tag{6.6}$$

$$\frac{1}{K(z)} \frac{\partial p}{\partial t} + \nabla \cdot \vec{\mathbf{u}} = 0. \tag{6.7}$$

We apply the Born approximation for the modeling of the scattering by the scatterer S [23]: the total field at the surface is the superposition of the primary field $(\vec{\mathbf{u}}_0, p_0)$ solution of

$$\rho_0 \frac{\partial \vec{\mathbf{u}}_0}{\partial t} + \nabla p_0 = \mathbf{f}^\varepsilon(t)\delta(\mathbf{x})\delta(z), \tag{6.8}$$

$$\frac{1}{K(z)}\frac{\partial p_0}{\partial t} + \nabla\cdot\vec{\mathbf{u}}_0 = 0 \tag{6.9}$$

determined here above (p_0 is given by (6.5)) and of a secondary field $(\vec{\mathbf{u}}_1, p_1)$ which originates from the emission of a secondary source located in S. The emission of the secondary source is proportional to the primary field at the position of the scatterer:

$$\rho_0 \frac{\partial \vec{\mathbf{u}}_1}{\partial t} + \nabla p_1 = -\rho_1 \mathbf{1}_B(\mathbf{x}, z)\frac{\partial \vec{\mathbf{u}}_0}{\partial t}, \tag{6.10}$$

$$\frac{1}{K(z)}\frac{\partial p_1}{\partial t} + \nabla\cdot\vec{\mathbf{u}}_1 = 0. \tag{6.11}$$

Taking a Fourier transform with respect to the time and the transverse spatial variables, the secondary system reads

$$-\rho_0 \frac{i\omega}{\varepsilon}\hat{\mathbf{v}}_1 + i\frac{\omega}{\varepsilon}\boldsymbol{\kappa}\hat{p}_1 = \rho_1 \frac{i\omega}{\varepsilon}\int \mathbf{v}_0(t,\mathbf{x},z)\mathbf{1}_B(\mathbf{x},z)e^{i\frac{\omega}{\varepsilon}(t-\boldsymbol{\kappa}\cdot\mathbf{x})}dtdx, \tag{6.12}$$

$$-\rho_0 \frac{i\omega}{\varepsilon}\hat{u}_1 + \frac{\partial \hat{p}_1}{\partial z} = \rho_1 \frac{i\omega}{\varepsilon}\int u_0(t,\mathbf{x},z)\mathbf{1}_B(\mathbf{x},z)e^{i\frac{\omega}{\varepsilon}(t-\boldsymbol{\kappa}\cdot\mathbf{x})}dtdx, \tag{6.13}$$

$$-\frac{1}{K(z)}\frac{i\omega}{\varepsilon}\hat{p}_1 + i\frac{\omega}{\varepsilon}\boldsymbol{\kappa}\cdot\hat{\mathbf{v}}_1 + \frac{\partial \hat{u}_1}{\partial z} = 0. \tag{6.14}$$

Assuming a point scatterer with scattering cross section $\varepsilon^3\sigma_s$,

$$\rho_1 \mathbf{1}_B(\mathbf{x}, z) = \varepsilon^3 \rho_0 \sigma_s \delta(\mathbf{x} - \mathbf{x}_s)\delta(z - z_s),$$

the total field writes

$$\vec{\mathbf{u}} = \vec{\mathbf{u}}_0 + \sigma_s \vec{\mathbf{u}}_1, \qquad p = p_0 + \sigma_s p_1,$$

where $(\vec{\mathbf{u}}_1, p_1)$ is solution of

$$-\rho_0 \frac{i\omega}{\varepsilon}\hat{\mathbf{v}}_1 + i\frac{\omega}{\varepsilon}\boldsymbol{\kappa}\hat{p}_1 = \mathbf{S}_{1,\mathbf{x}}(\omega)e^{-i\frac{\omega}{\varepsilon}\boldsymbol{\kappa}\cdot\mathbf{x}_s}\delta(z - z_s), \tag{6.15}$$

$$-\rho_0 \frac{i\omega}{\varepsilon}\hat{u}_1 + \frac{\partial \hat{p}_1}{\partial z} = S_{1,z}(\omega)e^{-i\frac{\omega}{\varepsilon}\boldsymbol{\kappa}\cdot\mathbf{x}_s}\delta(z - z_s), \tag{6.16}$$

$$-\frac{1}{K(z)}\frac{i\omega}{\varepsilon}\hat{p}_1 + i\frac{\omega}{\varepsilon}\boldsymbol{\kappa}\cdot\hat{\mathbf{v}}_1 + \frac{\partial \hat{u}_1}{\partial z} = 0, \tag{6.17}$$

with the secondary source terms given by

$$\mathbf{S}_{1,\mathbf{x}}(\omega) = \frac{i}{(2\pi)^2}\int \frac{\boldsymbol{\kappa}'}{2}\Big[R_g(\omega,\kappa',z_s)e^{i\frac{\omega}{\varepsilon}(\boldsymbol{\kappa}'\cdot\mathbf{x}_s + \zeta_0(\kappa')z_s)} - T_g(\omega,\kappa',z_s)e^{i\frac{\omega}{\varepsilon}(\boldsymbol{\kappa}'\cdot\mathbf{x}_s - \zeta_0(\kappa')z_s)}\Big]\hat{f}(\omega)\omega^3 d\boldsymbol{\kappa}', \tag{6.18}$$

$$S_{1,z}(\omega) = \frac{i}{(2\pi)^2}\int \frac{\rho_0}{2I_0(\kappa')}\Big[R_g(\omega,\kappa',z_s)e^{i\frac{\omega}{\varepsilon}(\boldsymbol{\kappa}'\cdot\mathbf{x}_s + \zeta_0(\kappa')z_s)} + T_g(\omega,\kappa',z_s)e^{i\frac{\omega}{\varepsilon}(\boldsymbol{\kappa}'\cdot\mathbf{x}_s - \zeta_0(\kappa')z_s)}\Big]\hat{f}(\omega)\omega^3 d\boldsymbol{\kappa}'. \tag{6.19}$$

Note that this source term corresponds to the emission of a point source similar to the embedded source problem (2.1-2.3). Applying a stationary phase argument we can get a simpler form of the source term $\vec{\mathbf{S}}_1$:

$$\vec{\mathbf{S}}_1 = -\frac{\varepsilon}{(2\pi)^2}\frac{\omega^2\pi|z_s|}{c_0^2|OS|^3}\vec{OS}\left(T_g(\omega,\mu_c',z_s)e^{i\frac{\omega}{\varepsilon}\frac{|OS|}{c_0}} - R_g(\omega,\mu_c',z_s)e^{-i\frac{\omega}{\varepsilon}\frac{|OS|}{c_0}}\right)\hat{f}(\omega),$$

with $\mu_c' = |\mathbf{x}_s|/(c_0|OS|)$. We actually keep the integral representation of $\vec{\mathbf{S}}_1$ as we shall apply the stationary phase argument only once the final integral expression of the observed signal is obtained. Let us consider the secondary pressure field p_1 at the observation point $O_1 = (\mathbf{x}_1, 0)$. We get that p_1 consists of four terms. The first one is

$$p_{1,I}(t_0+\varepsilon\sigma,\mathbf{x}_1) = \frac{1}{(2\pi)^5\varepsilon}\frac{i}{4}\int T_g(\omega,\kappa,z_s)T_g(\omega,\kappa',z_s)\left(-\frac{I_0(\kappa)\boldsymbol{\kappa}\cdot\boldsymbol{\kappa}'}{\rho_0}+\frac{\rho_0}{I_0(\kappa')}\right)$$
$$\times e^{-i\omega\sigma}e^{i\frac{\omega}{\varepsilon}\phi_I(\boldsymbol{\kappa},\boldsymbol{\kappa}')}\hat{f}(\omega)\omega^5 d\boldsymbol{\kappa}d\boldsymbol{\kappa}'d\omega, \tag{6.20}$$

where the rapid phase is

$$\phi_I(\boldsymbol{\kappa},\boldsymbol{\kappa}') = -t_0 + \boldsymbol{\kappa}\cdot\mathbf{x}_1 - \zeta_0(\kappa)z_s - \boldsymbol{\kappa}\cdot\mathbf{x}_s + \boldsymbol{\kappa}'\cdot\mathbf{x}_s - \zeta_0(\kappa')z_s.$$

The three other terms $p_{1,II}$, $p_{1,III}$, and $p_{1,IV}$ have similar expressions but with crossed products R_gT_g, T_gR_g, and R_gR_g, respectively, and rapid phases with different signs in front of $\zeta_0(\kappa)z_s$ and $\zeta_0(\kappa')z_s$.

We take polar coordinates and parameterize $\mathbf{x}_s = |\mathbf{x}_s|\mathbf{e}_{\theta_s}$, $\mathbf{x}_1 = \mathbf{x}_s + |\mathbf{x}_1 - \mathbf{x}_s|\mathbf{e}_{\bar{\theta}}$. We apply a stationary phase argument and find that there exists a stationary map given by

$$\mu_c' = \frac{1}{c_0}\frac{|\mathbf{x}_s|}{\sqrt{|\mathbf{x}_s|^2+z_s^2}}, \quad \mu_c = \frac{1}{c_0}\frac{|\mathbf{x}_1-\mathbf{x}_s|}{\sqrt{|\mathbf{x}_1-\mathbf{x}_s|^2+z_s^2}}, \quad \theta_c' = \theta_s, \quad \theta_c = \bar{\theta},$$

only if $t_0 = t_c$ with

$$t_c = \frac{1}{c_0}\left(\sqrt{|\mathbf{x}_s|^2+z_s^2}+\sqrt{|\mathbf{x}_1-\mathbf{x}_s|^2+z_s^2}\right) = \frac{1}{c_0}\left(|OS|+|O_1S|\right). \tag{6.21}$$

We then find that, to leading order in ε,

$$p_{1,I}(t_0+\varepsilon\sigma,\mathbf{x}_1) = \frac{1}{(2\pi)^3}\frac{i}{4}\frac{|z_s|}{c_0^3}\frac{\vec{OS}\cdot\vec{SO}_1}{|OS|^3|SO_1|^2}$$
$$\times\int T_g(\omega,\mu_c,z_s)T_g(\omega,\mu_c',z_s)e^{-i\omega\sigma}\hat{f}(\omega)\omega^3 d\omega. \tag{6.22}$$

We also find that the three other terms $p_{1,II}$, $p_{1,III}$, and $p_{1,IV}$ do not have such a stationary map, so that they bring a contribution to the value of p_1 which is at least of order $\sqrt{\varepsilon}$ lower than $p_{1,I}$.

We finally apply the same asymptotic analysis as in Section 5, so as to obtain the statistical limit of the product $T_g(\omega,\mu_c,z_s)T_g(\omega,\mu_c',z_s)$. Besides we have established in Proposition 6.1 that the primary field p_0 is vanishing at the surface. Combining these results we establish the following proposition.

PROPOSITION 6.2. *Let t_c be equal to (6.21). If $t_0 \neq t_c$, then the pressure field $p(t_0+\varepsilon\cdot)$ at the observation point $O_1 = (\mathbf{x}_1, 0)$ converges to 0. If $t_0 = t_c$, then the*

pressure field converges in distribution to a random function

$$p(t_c+\varepsilon\sigma) \overset{\varepsilon\to 0}{\longrightarrow} \frac{1}{(2\pi)^3}\frac{i}{4}\frac{\sigma_s|z_s|}{c_0^3}\frac{\vec{OS}\cdot\vec{SO_1}}{|OS|^3|SO_1|^2} \tag{6.23}$$
$$\times\int \hat{f}(\omega)\exp\left[i\omega\left(\frac{1}{c_0}\frac{\sqrt{\gamma_0}}{\sqrt{2}}\frac{|OS|+|SO_1|}{|z_s|}B_{z_s}-\sigma\right)-\omega^2\left(\frac{\gamma_0}{4c_0^2}\frac{|OS|^2+|SO_1|^2}{|z_s|}\right)\right]\omega^3 d\omega,$$

where B is a standard Brownian motion that is independent of the observation point. This means that the field at the observation point has a deterministic shape given by the inverse Fourier transform of

$$\frac{1}{(2\pi)^3}\frac{i}{4}\frac{\sigma_s|z_s|}{c_0^3}\frac{\vec{OS}\cdot\vec{SO_1}}{|OS|^3|SO_1|^2}\hat{f}(\omega)\exp\left[-\omega^2\left(\frac{\gamma_0}{4c_0^2}\frac{|OS|^2+|SO_1|^2}{|z_s|}\right)\right]\omega^3.$$

This deterministic shape is thus the convolution of the original pulse shape of the source with a deterministic kernel. The field has also a random center that is given by

$$T_1=\frac{1}{c_0}\left(|OS|+|O_1S|\right)\left(1+\varepsilon\frac{\sqrt{\gamma_0}}{\sqrt{2}}\frac{1}{|z_s|}B_{z_s}\right) \tag{6.24}$$

Note that the pressure field consists only on the scattered field $\sigma_s p_1$, as we have proved in Proposition 6.1 that the primary field generated by the source is a pure longitudinal velocity field at the surface. Concerning the longitudinal velocity field, we have the following result.

PROPOSITION 6.3. *If $c_0t_0 \notin \{|OO_1|, |OS|+|OO_1|\}$, then the field $u(t_0+\varepsilon\cdot)$ at the observation point $O_1=(\mathbf{x}_1,0)$ converges to 0. If $c_0t_0=|OO_1|$, then the field $u(t_0+\varepsilon\cdot,\mathbf{x}_1,0)$ converges in probability to the deterministic function*

$$u(t_0+\varepsilon\sigma)\overset{\varepsilon\to 0}{\longrightarrow} -\frac{1}{4\pi^2\rho_0c_0|OO_1|^2}f(\sigma)$$

If $c_0t_0=|OS|+|SO_1|$, then the field $u(t_0+\varepsilon\cdot,\mathbf{x}_1,0)$ converges in distribution to a random function

$$u(t_0+\varepsilon\sigma)\overset{\varepsilon\to 0}{\longrightarrow} \frac{1}{(2\pi)^3}\frac{i}{4}\frac{\sigma_s z_s^2}{\rho_0c_0^4}\frac{\vec{OS}\cdot\vec{SO_1}}{|OS|^3|SO_1|^3} \tag{6.25}$$
$$\times\int \hat{f}(\omega)\exp\left[i\omega\left(\frac{1}{c_0}\frac{\sqrt{\gamma_0}}{\sqrt{2}}\frac{|OS|+|SO_1|}{|z_s|}B_{z_s}-\sigma\right)-\omega^2\left(\frac{\gamma_0}{4c_0^2}\frac{|OS|^2+|SO_1|^2}{|z_s|}\right)\right]\omega^3 d\omega$$

where B is a standard Brownian motion that is independent of the observation point. The first time ($t_0=|OO_1|/c_0$) corresponds to the arrival time of the direct primary field. The second time ($t_0=(|OS|+|SO_1|)/c_0$) corresponds to the expected arrival time of the secondary scattered field.

Assume that we have four observation points O_j, $j=1,\cdots,4$. From the recorded signals we are able to detect the four arrival times T_j of the secondary front pulses for each observation point O_j, $j=1,\cdots,4$,

$$T_j=\frac{1}{c_0}\left(|O_jS|+|OS|\right)\left(1+Z_s\right), \tag{6.26}$$

with $Z_s=\varepsilon\sqrt{\gamma_0/2}B_{z_s}/|z_s|$. The analysis has shown that Z_s does not depend on the observation points. We can propose a way to compute the scatterer location that is error-free. Indeed, the scatterer location S and the random delay Z_s satisfy the four independent relations (6.26) and can thus be inverted from the arrival times T_j.

6.2. Illumination by a source emitting a stationary random signal. A source located at the surface at $(\mathbf{0}, 0)$ emits a stationary random signal of the form

$$\vec{\mathbf{f}}^{\varepsilon}(t) = \varepsilon^{\frac{1}{2}} \begin{pmatrix} \mathbf{0} \\ 1 \end{pmatrix} f(\frac{t}{\varepsilon}),$$

where f is a stationary random process with power spectral density $\hat{\mathcal{G}}$

$$f(t) = \frac{1}{\sqrt{2\pi}} \int \sqrt{\hat{\mathcal{G}}}(\omega) e^{i\omega t} dW_\omega.$$

W_ω a $\mathbb{C}$-valued Gaussian process

$$W_\omega = \frac{W^1_\omega + W^1_{-\omega}}{2} + i \frac{W^2_\omega - W^2_{-\omega}}{2}$$

where W^1 and W^2 are two independent one-dimensional Brownian motions. In absence of scatterer, the pressure field at the surface is

$$p_0(t, \mathbf{x}) = \frac{1}{(2\pi)^{\frac{5}{2}} \varepsilon^{\frac{3}{2}}} \int \frac{1 - R(\omega, \kappa, -L, 0)}{2} e^{-i\frac{\omega}{\varepsilon}(t - \boldsymbol{\kappa}\cdot\mathbf{x})} \sqrt{\hat{\mathcal{G}}}(\omega) \omega^2 d\boldsymbol{\kappa} dW_\omega. \tag{6.27}$$

The field at a position $(\mathbf{x}_s, z_s)$ inside the medium $(z_s < 0)$ is

$$\begin{aligned} p_0(t, \mathbf{x}_s, z_s) = \frac{1}{(2\pi)^{\frac{5}{2}} \varepsilon^{\frac{3}{2}}} \int \Bigg[& \frac{R_g(\omega, \kappa, z_s)}{2} e^{-i\frac{\omega}{\varepsilon}(t - \boldsymbol{\kappa}\cdot\mathbf{x}_s - \zeta_0(\kappa) z_s)} \\ & - \frac{T_g(\omega, \kappa, z_s)}{2} e^{-i\frac{\omega}{\varepsilon}(t - \boldsymbol{\kappa}\cdot\mathbf{x}_s + \zeta_0(\kappa) z_s)} \Bigg] \sqrt{\hat{\mathcal{G}}}(\omega) \omega^2 d\boldsymbol{\kappa} dW_\omega. \end{aligned} \tag{6.28}$$

We now consider a scatterer embedded at $S = (\mathbf{x}_s, z_s)$. Applying the Born approximation, the total field at the surface is the superposition of the primary field p_0 given by (6.27) and of the secondary field which originates from the emission of the secondary source located in S. We consider in this section the CCF of the signals recorded at two observation points O_1 and O_2 located at the surface:

$$C(t_0 + \varepsilon\sigma) = \int p(t, \mathbf{x}_1, 0) p(t + t_0 + \varepsilon\sigma, \mathbf{x}_2, 0) G(t) dt \tag{6.29}$$

for some cut-off function G. Using the same methodology as in Section 5 we prove the following proposition.

PROPOSITION 6.4. *Let t_c be equal to*

$$t_c = \frac{1}{c_0} \left(|SO_2| - |SO_1| \right). \tag{6.30}$$

If $t_0 \neq t_c$, then the CCF converges to 0. If $t_0 = t_c$, then the CCF converges in distribution to a random function

$$\begin{aligned} C(t_c + \varepsilon\sigma) \xrightarrow{\varepsilon \to 0} & \frac{1}{16(2\pi)^5} \frac{\sigma_s^2 |z_s|^2}{c_0^6} \frac{\vec{OS}\cdot\vec{SO_1}\ \vec{OS}\cdot\vec{SO_2}}{|OS|^6 |SO_1|^2 |SO_2|^2} \bar{G} \\ & \times \int \hat{\mathcal{G}}(\omega) \exp\left[i\omega \left(\frac{1}{c_0} \frac{\sqrt{\gamma_0}}{\sqrt{2}} \frac{|SO_1| - |SO_2|}{|z_s|} B_{z_s} + \sigma \right) \right] K(\omega) d\omega, \end{aligned} \tag{6.31}$$

where $\bar{G} = \int G(t)dt$, *B is a standard Brownian motion that is independent of the observation point,*

$$K(\omega) = \exp\left[-\omega^2\left(\frac{\gamma_0}{4c_0^2}\frac{|SO_2|^2+|SO_1|^2}{|z_s|}\right)\right] \times W_{g,1}\left(\omega, \frac{1}{c_0}\frac{|\mathbf{x}_s|}{|OS|}, z_s\right)\omega^6,$$

and $W_{g,1}$ *is given by (5.10).*

This means that the CCF has a deterministic shape given by the inverse Fourier transform of

$$\frac{1}{16(2\pi)^5}\frac{\sigma_s^2|z_s|^2}{c_0^6}\frac{\vec{OS}\cdot\vec{SO}_1\ \vec{OS}\cdot\vec{SO}_2}{|OS|^6|SO_1|^2|SO_2|^2}\hat{\mathcal{G}}(\omega)K(\omega)\bar{G}.$$

This deterministic shape is thus the convolution of the original power spectral density of the source with a deterministic kernel. Note that the kernel is more complicated than the ones that have been exhibited in the previous sections, because it involves the expectation of a product of the form $\overline{T_g}(\mu_c',\omega)\overline{T_g}(\mu_c,\omega)T_g(\mu_c,\omega)T_g(\mu_c'',\omega)$ with $\mu \neq \mu_c' \neq \mu_c'$. The presence of two correlated generalized transmission coefficients (those with the same μ) is the origin of the complicated kernel. The CCF has also a random center that is given by

$$T_{21} = \frac{1}{c_0}\left(|O_2S| - |O_1S|\right)\left(1 + \varepsilon\frac{\sqrt{\gamma_0}}{\sqrt{2}}\frac{1}{|z_s|}B_{z_s}\right). \tag{6.32}$$

The procedure to identify the scatterer location is the same as the one described in Subsection 5.6 and requires the CCF between five observation points, O_j, $j = 1, \cdots, 5$. By observing the maxima T_{j5} of the CCF between O_j and O_5, we get the scatterer location S and the random delay by inverting the four relations

$$(|O_jS| - |O_5S|)(1 + Z_s) = c_0T_{j5}, \quad j = 1, \cdots, 4.$$

6.3. Illumination by a set of random sources. We assume in this section a series of sources located at the surface and generating random signals. These signals are assumed to be independent and the positions of the sources are denoted by $S_j = (\mathbf{x}_{sj}, 0)$, $j = 1, \cdots, n$. The total source term is therefore

$$\vec{\mathbf{F}}^{\varepsilon}(t,\mathbf{x},z) = \varepsilon^{\frac{1}{2}}\sum_{j=1}^{n}\begin{pmatrix}\mathbf{0}\\1\end{pmatrix}f_j(\frac{t}{\varepsilon})\delta(\mathbf{x}-\mathbf{x}_{sj})\delta(z),$$

where f_j are independent processes with power spectral densities $\hat{\mathcal{G}}_j$. The results obtained in the previous subsection can be readily extended to this configuration. We consider a scatterer located in $S = (\mathbf{x}_s, z_s)$ and two observation points $O_1 = (\mathbf{x}_1, 0)$ and $O_2 = (\mathbf{x}_2, 0)$. We compute the CCF defined by (6.29).

PROPOSITION 6.5. *Let* t_c *be equal to (6.30). If* $t_0 \neq t_c$, *then the CCF* $C(t_0 + \varepsilon\cdot)$ *converges to* 0. *If* $t_0 = t_c$, *then the CCF* $C(t_c + \varepsilon\cdot)$ *converges in distribution to a random function*

$$C(t_c + \varepsilon\sigma) \overset{\varepsilon\to 0}{\longrightarrow} \overline{C}(\sigma - T), \tag{6.33}$$

whose shape is deterministic but the center is randomly shifted. The shape is

$$\overline{C}(\sigma) = \frac{1}{16(2\pi)^5}\frac{\sigma_s^2|z_s|^2}{c_0^6}\sum_{j=1}^{n}\frac{\vec{S_jS}\cdot\vec{SO}_1\ \vec{S_jS}\cdot\vec{SO}_2}{|S_jS|^6|SO_1|^2|SO_2|^2}\bar{G}\int\hat{\mathcal{G}}_j(\omega)e^{i\omega\sigma}K_j(\omega)d\omega,$$

with $\bar{G} = \int G(t)dt$,

$$K_j(\omega) = \exp\left[-\omega^2\left(\frac{\gamma_0}{4c_0^2}\frac{|SO_2|^2+|SO_1|^2}{|z_s|}\right)\right] \times W_{g,1}\left(\omega, \frac{1}{c_0}\frac{|\mathbf{x}_{sj}-\mathbf{x}_s|}{|S_jS|}, z_s\right)\omega^6,$$

and $W_{g,1}$ *is given by (5.10). The random center is*

$$T = \frac{1}{c_0}\frac{\sqrt{\gamma_0}}{\sqrt{2}}\frac{|SO_2|-|SO_1|}{|z_s|}B_{z_s},$$

where B *is a standard Brownian motion that is independent of the observation point.*

We could consider a series of sources located at the surface or inside the medium emitting more complicated signals. This would modify the deterministic shape of the CCF, but not the statistical properties of the center of the CCF. Accordingly the imaging procedure proposed in the previous subsection can be applied to the detection of an embedded object by cross-correlating the random noises recorded at five observation points.

7. Conclusion. In this paper we have analyzed the statistical properties of the signal recorded at the surface and emitted by a source embedded in a randomly layered half-space. We have proposed a procedure to locate the source that removes the random components introduced by the multiple scattering in the medium and thus allows an exact localization without knowing the medium. We have extended this work for the imaging of passive scatterers embedded in a random half-space and illuminated by a source located at the surface or simply by random noise generated by a set of unknown sources. We have shown that the cross-correlation function of the noisy signals recorded at two observation points on the surface can be used to retrieve information about ballistic motion. This information can be processed for imaging. We have proved that the method is stable with respect to the statistical distribution of the medium and with respect to the statistical distribution of the noisy sources. It enables a passive way of imaging an unknown medium by using only background noise. For instance, we may think that it could provide a way of building "pseudo-seismograms" in geophysics where controlled active sources are difficult to achieve.

Acknowledgments. The author would like to thank J.-P. Fouque, K. Solna, and A. Nachbin for stimulating discussions. The author also acknowledges support by the French Ministry of Research ACI-NIM-2003-94.

Appendix A. Statistical properties of the reflection and transmission coefficients.

A.1. Moments at different slowness vectors. The values of the moments of the transmission coefficient at different slowness vectors is required in Section 5.3. Let us consider $z_0 < z_1$, a frequency ω, and $n + n'$ different slowness vector moduli $\kappa_1 \neq ... \neq \kappa_n \neq \kappa'_1 \neq ... \neq \kappa'_{n'}$. The computation of the limits of the moments

$$\lim_{\varepsilon\to 0}\mathbb{E}\left[\prod_{j=1}^{n} T(\omega,\kappa_j,z_0,z_1)\prod_{j=1}^{n'}\overline{T}(\omega,\kappa'_j,z_0,z_1)\right]$$

has been carried out in [9]. It is found that the limits are

$$\mathbb{E}\left[\prod_{j=1}^{n} T_{\text{eff}}(\omega,\kappa_1,z_0,z_1)\prod_{j=1}^{n'}\overline{T_{\text{eff}}}(\omega,\kappa'_j,z_0,z_1)\right],$$

where

$$T_{\rm eff}(\omega,\kappa,z_0,z)=\exp\left(i\sqrt{\gamma(\omega,\kappa)}(B_{z_0}-B_z)+\frac{\gamma(\omega,\kappa)(z_0-z)}{2}\right),$$

and B is a standard one-dimensional Brownian motion. The same computation carried out with the reflection coefficient leads to the limit

$$\lim_{\varepsilon\to 0}\mathbb{E}\left[\prod_{j=1}^{n}R(\omega,\kappa_j,z_0,z_1)\prod_{j=1}^{n'}\overline{R}(\omega,\kappa_j',z_0,z_1)\right]=0.$$

A.2. Moments with the same slowness vector. As shown in [1, 7] we have, for $z_0\le z$,

$$\mathbb{E}\left[R^n(\omega,\kappa,z_0,z)\overline{R}^m(\omega,\kappa,z_0,z)\right]\stackrel{\varepsilon\to 0}{\longrightarrow}\left\{\begin{array}{ll}W_n(\omega,\kappa,z_0,z) & \text{if } m=n,\\ 0 & \text{otherwise,}\end{array}\right.$$

where the quantity W_n is obtained through the following system of equations:

$$\begin{aligned}&\frac{\partial W_n}{\partial z}=\gamma(\omega,\kappa)n^2\left(W_{n+1}+W_{n-1}-2W_n\right),\\ &W_n(\omega,\kappa,z_0,z=z_0)=\mathbf{1}_0(n).\end{aligned}$$

Denoting $U_j^\varepsilon=R(\omega_j,\mu_j,z_0,z)\overline{R}(\omega_j,\mu_j,z_0,z)$, it is shown in [7] that for two distinct frequencies $\omega_1\neq\omega_2$ or for distinct $\mu_1\neq\mu_2$ we have

$$\left|\mathbb{E}\left[U_1^\varepsilon U_2^\varepsilon\right]-\mathbb{E}\left[U_1^\varepsilon\right]\mathbb{E}\left[U_2^\varepsilon\right]\right|\stackrel{\varepsilon\to 0}{\longrightarrow}0. \tag{A.1}$$

This decorrelation property is used in Section 5.3 to deduce the self-averaging property of the refocused pulse. Cross-moments of transmission and reflection coefficients are also required in Section 5.3. Using once again the results contained in [1], we get that

$$\mathbb{E}\left[R^nT(\omega,\kappa,z_0,z)\overline{R^mT}(\omega,\kappa,z_0,z)\right]\stackrel{\varepsilon\to 0}{\longrightarrow}\left\{\begin{array}{ll}\widetilde{W}_n(\omega,\kappa,z_0,z) & \text{if } m=n,\\ 0 & \text{otherwise,}\end{array}\right.$$

where the quantity $\widetilde{W}_n$ is obtained through the following system of equations:

$$\begin{aligned}&\frac{\partial\widetilde{W}_n}{\partial z}=\gamma(\omega,\kappa)\left((n+1)^2\widetilde{W}_{n+1}+n^2\widetilde{W}_{n-1}-(n^2+(n+1)^2)\widetilde{W}_n\right),\\ &\widetilde{W}_n(\omega,\kappa,z_0,z=z_0)=\mathbf{1}_0(n).\end{aligned}$$

REFERENCES

[1] M. Asch, W. Kohler, G. Papanicolaou, M. Postel, and B. White, Frequency content of randomly scattered signals, SIAM Rev. **33** (1991) 519-625.
[2] A. B. Baggeroer, W. A. Kuperman, and P. N. Mikhalevsky, An overview of matched field methods in ocean acoustics, IEEE Ocean. Eng. **18** (1993) 401-424.
[3] G. Bal, G. Papanicolaou, and L. Ryzhik, Self-averaging in time reversal for the parabolic wave equation, Stochastics and Dynamics **2** (2002) 507-531.
[4] L. Berlyand and R. Burridge, The accuracy of the O'Doherty-Anstey approximation for wave propagating in highly disordered stratified media, Wave Motion **21** (1995) 357-373.
[5] P. Blomgren, G. Papanicolaou, and H. Zhao, Super-resolution in time-reversal acoustics, J. Acoust. Soc. Am. **111** (2002) 230-248.

[6] L. Borcea, C. Tsogka, G. Papanicolaou and J. Berryman, Imaging and time reversal in random media, Inverse Problems **18** (2002) 1247-1279.
[7] R. Burridge, G. Papanicolaou, and B. White, Statistics for pulse reflection from a randomly layered medium, SIAM J. Appl. Math. **47** (1987) 146-168.
[8] M. Campillo and A. Paul, Long range correlations in the seismic coda, Science **29** (2003) 547-549.
[9] J. Chillan and J.-P. Fouque, Pressure fields generated by acoustical pulses propagating in randomly layered media, SIAM J. Appl. Math. **58** (1998) 1532-1546.
[10] J.-F. Clouet and J.-P. Fouque, Spreading of a pulse traveling in random media, Ann. Appl. Probab. **4** (1994) 1083-1097.
[11] J.-F. Clouet and J.-P. Fouque, A time-reversal method for an acoustical pulse propagating in randomly layered media, Wave Motion **25** (1997) 361-368.
[12] M. D. Collins and W. A. Kuperman, Focalization: environmental focusing and source localization, J. Acoust. Soc. Am. **90** (1991) 1410-1422.
[13] T. L. Duvall Jr., S. M. Jefferies, J. W. Harvey, and M. A. Pomerantz, Time-distance helioseismology, Nature **362** (1993) 430-432.
[14] M. R. Fallat and S. E. Dosso, Geoacoustic inversion for the Workshop97 benchmark test cases using simulated annealing, J. Comput. Acoust. **6** (1998) 29-43.
[15] M. Fink, Time reversal mirrors, J. Phys. D: Appl. Phys. **26** (1993) 1333-1350.
[16] M. Fink, Time reversed acoustics, Scientific American **285**:5 (1999) 91-97.
[17] J.-P. Fouque, J. Garnier, A. Nachbin, and K. Sølna, Time reversal refocusing for point source in randomly layered media, submitted (2004).
[18] J.-P. Fouque and K. Sølna, Time-reversal aperture enhancement, SIAM Multiscale Modeling and Simulation **1** (2003) 239-259.
[19] P. Gerstoft, Inversion of seismoacoustic data using genetic algorithms and a posteriori probability distributions, J. Acoust. Soc. Am. **95** (1994) 770-782.
[20] P. Gerstoft, Inversion of acoustic data using a combination of genetic algorithms and the Gauss-Newton approach, J. Acoust. Soc. Am. **97** (1995) 2181-2190.
[21] P. Lewicki, R. Burridge, and G. Papanicolaou, Pulse stabilization in a strongly heterogeneous medium, Wave Motion **20** (1994) 177-195.
[22] A. E. Malcolm, J. Scales, and B. A. van Tiggelen, Extracting the Green function from diffuse, equipartitioned waves, Phys. Rev. E **70**, 015601(2004).
[23] P. M. Morse and K. U. Ingard, *Theoretical acoustics*, McGraw-Hill, New York, 1968.
[24] R. F. O'Doherty and N. A. Anstey, Reflections on amplitudes, Geophysical Prospecting **19** (1971) 430-458.
[25] J. Rickett and J. Claerbout, Passive seismic imaging applied to synthetic data, Stanford Exploration Project, Report 92, November 1997, pp. 87-91.
[26] P. Roux and M. Fink, Green's function estimation using secondary sources in a shallow water environment, J. Acoust. Soc. Am. **133** (2003) 1406-1416.
[27] M. K. Sen and P. L. Stoffa, *Global optimization methods in geophysical inversion*, Elsevier, Amsterdam, 1995.
[28] M. Siderius, P. L. Nielsen, J. Sellschoop, M. Snellen, and D. Simons, Experimental study of geoacoustic inversion uncertainty due to ocean sound-speed fluctuations, J. Acoust. Soc. Am. **110** (2001) 769-781.
[29] M. Snellen, D. G. Simons, M. Siderius, J. Sellschoop, and P. L. Nielsen, An evaluation of the accuracy of shallow water matched field inversion results, J. Acoust. Soc. Am. **109** (2001) 514-527.
[30] R. Snieder, Imaging and averaging in complex media, in Diffusive wave in complex media, J.-P. Fouque, ed., NATO Science Series C, Vol. 531, Kluwer, 1999, pp. 405-454.
[31] R. Snieder, Extracting the Green's function from the correlation of coda waves: A derivation based on stationary phase, Phys. Rev. E **69** (2004), 046610.
[32] K. Sølna and G. Papanicolaou, Ray theory for a locally layered medium, Waves in Random Media **10** (2000) 151-198.
[33] A. Tarantola, *Inverse problem theory: Methods for data fitting and model parameter estimation*, Elsevier, Amsterdam, 1987.
[34] A. Tolstoy, *Matched field processing for underwater acoustics*, World Scientific, Singapore, 1993.
[35] R. Weaver and O. I. Lobkis, Ultrasonics without a source: Thermal fluctuation correlations at MHz frequencies, Phys. Rev. Lett. **84** (2001), 134301.